First-Principles Elucidation and Design of Catalytic and Electrocatalytic Materials

Progress, Challenges and Perspectives

Matthew Neurock

Departments of Chemical Engineering and Chemistry
University of Virginia, Charlottesville, VA

PNNL Workshop 2006

Can We Mimic Nature?

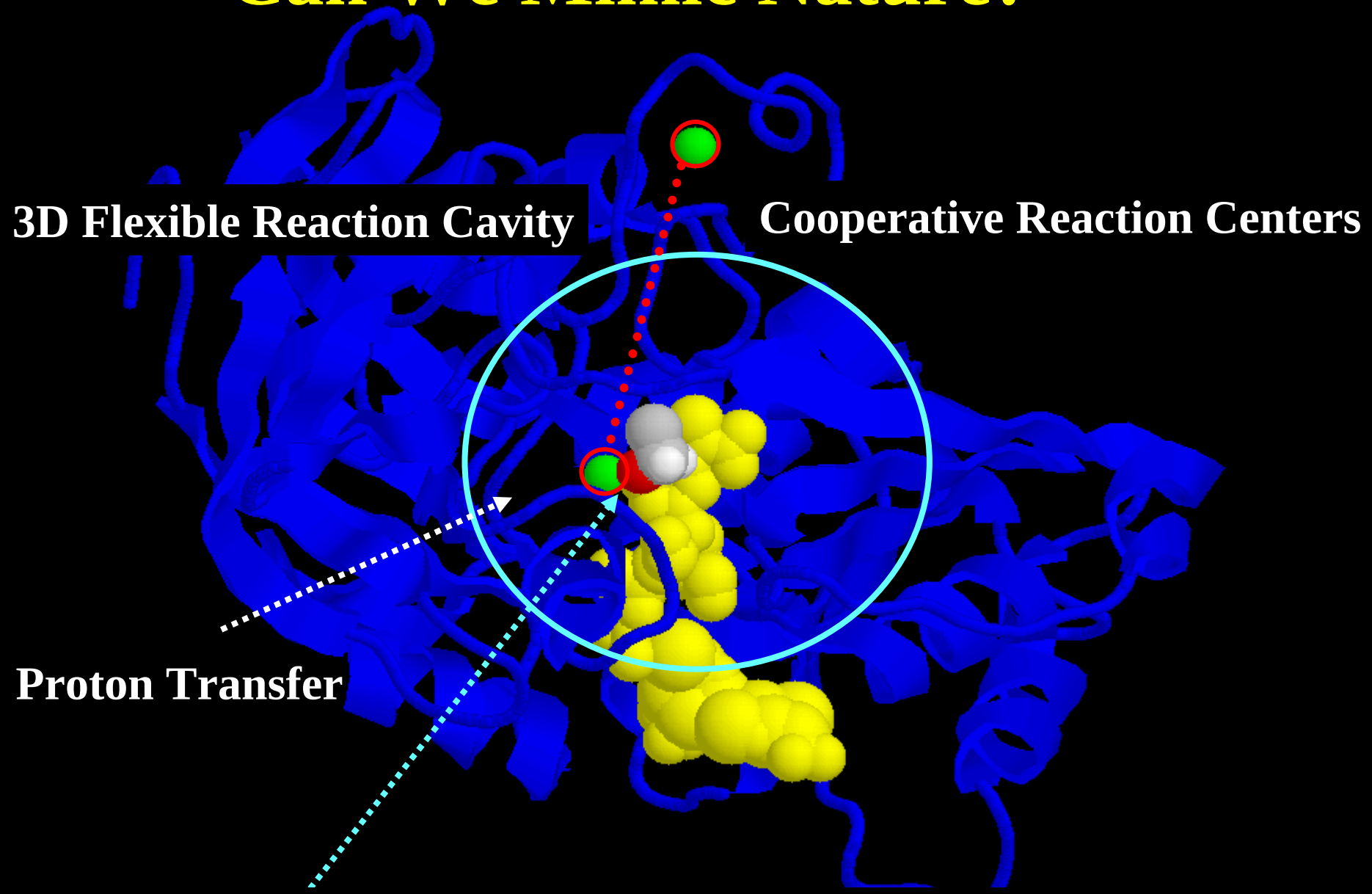

Supported Metal Catalysts

3D Particles But Largely 2D Chemistry

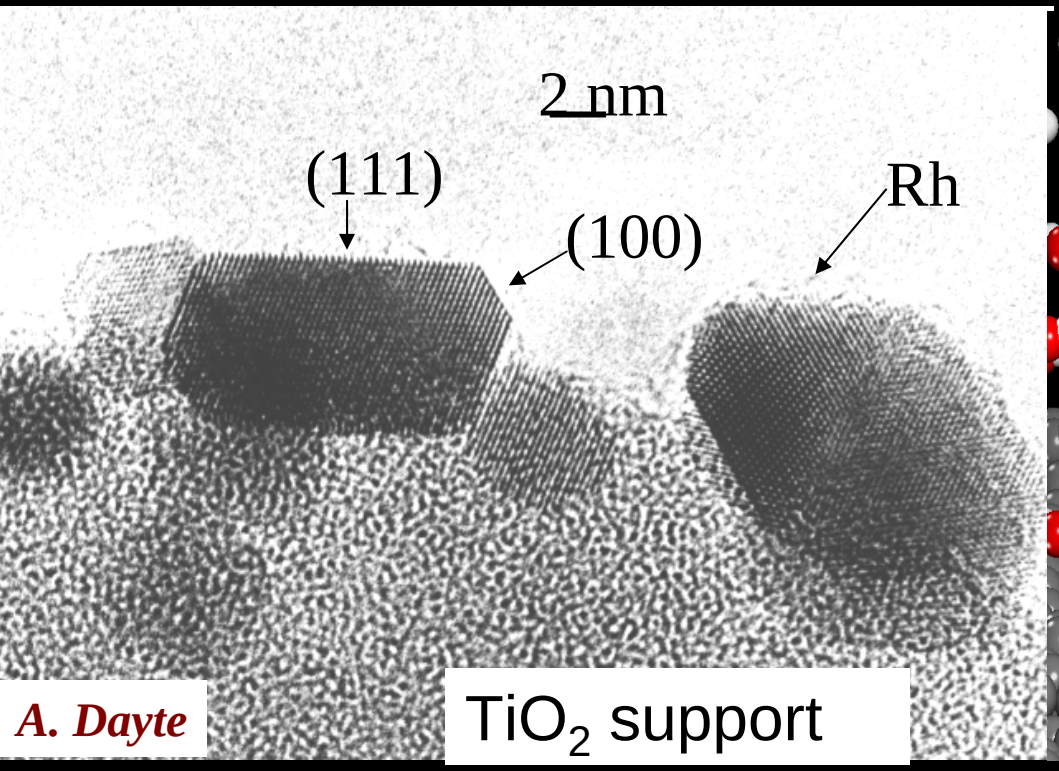

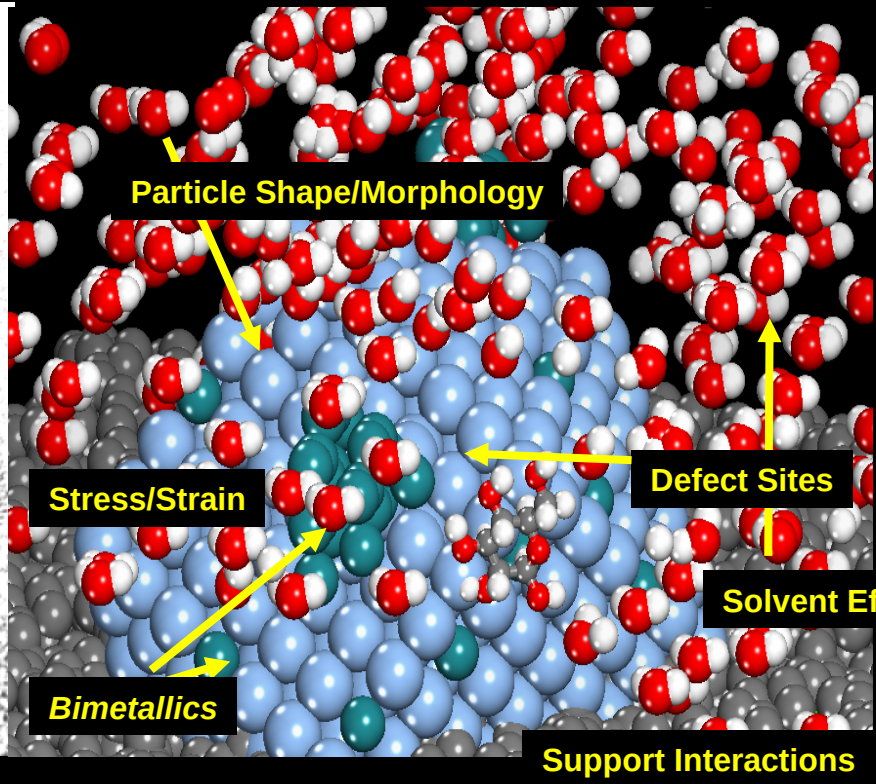

Inorganic Materials - Limited Flexibility

Engineering the Reaction Environment

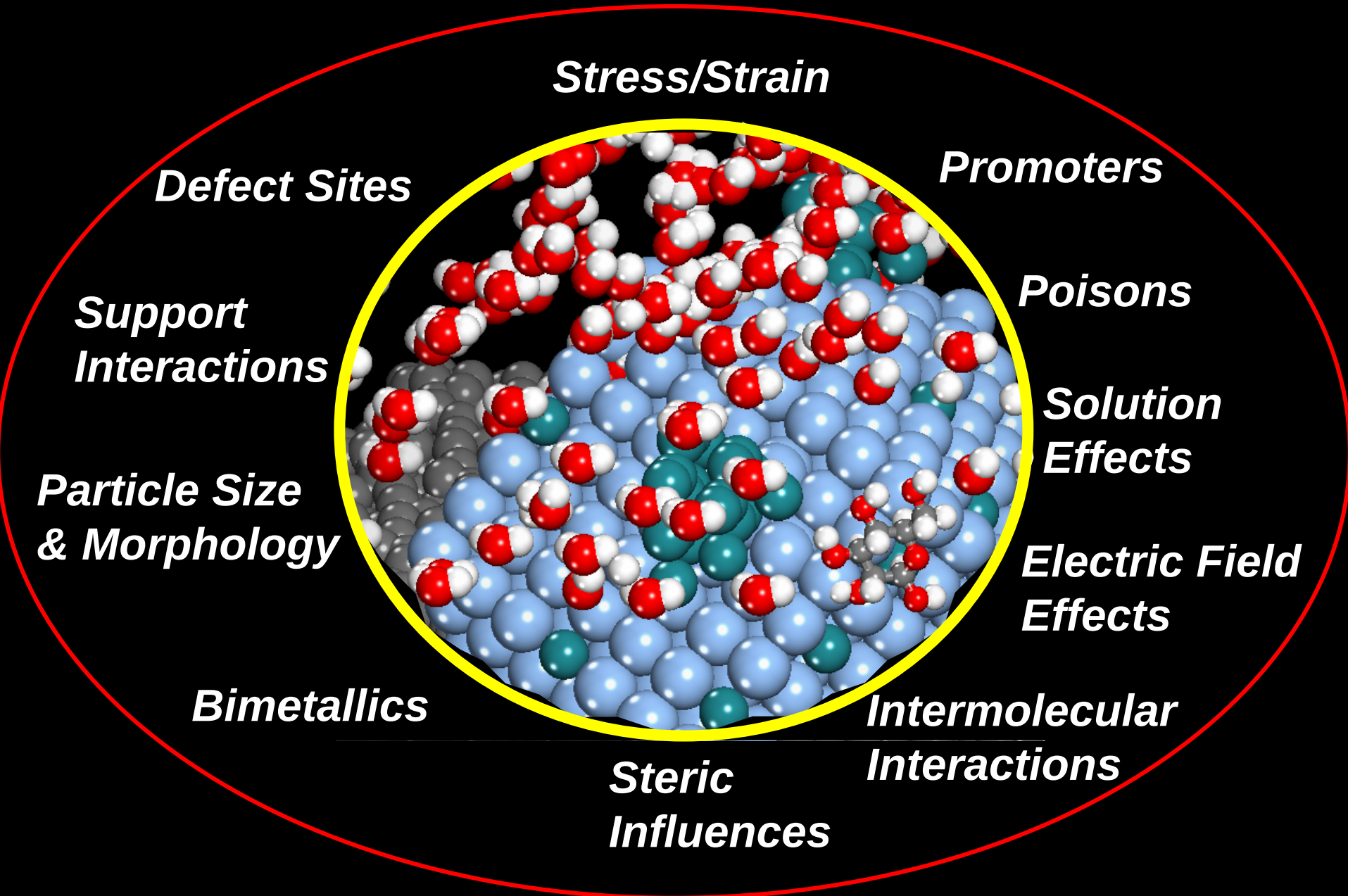

Multiscale Modeling

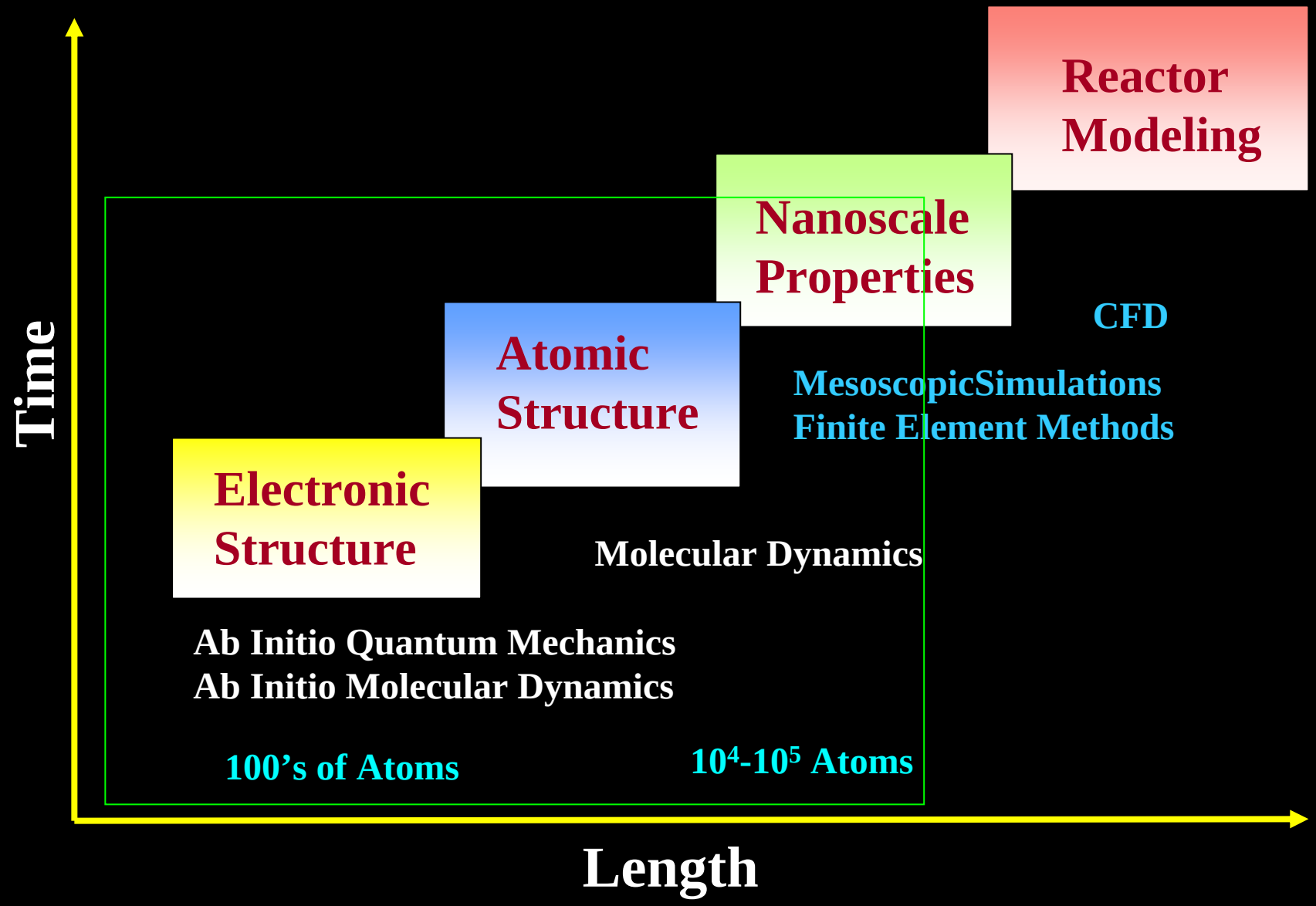

Computational Catalysis

Where Are We Today?

Prediction of Structure, Spectroscopy, and Reaction Energetics

Elucidate Mechanism

Initial Stages of Catalyst Design

Metals, Composition, Support, Surface Structure, Promoters

Property Predictions

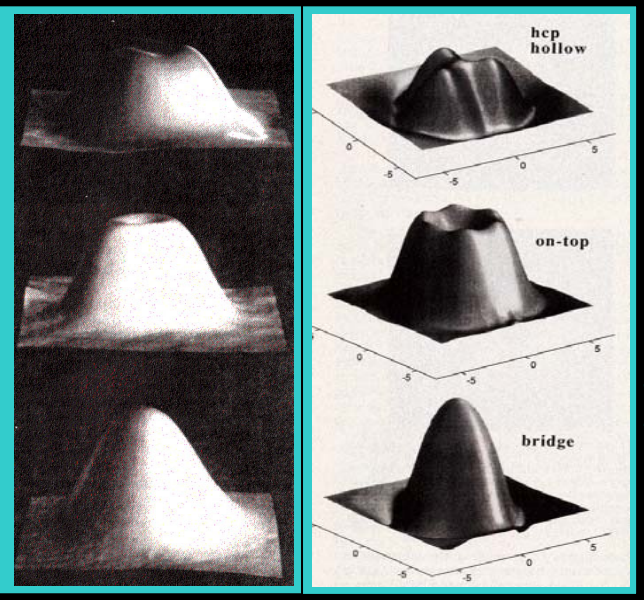

P. Sautet, Chem. Rev., 97, 1097, 1997.

Structure (0.05 Å)

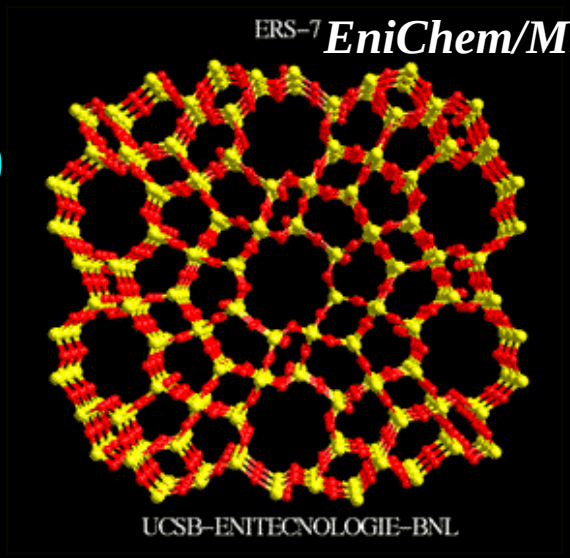

STM (qualitative)
Optical (UV 0.5eV)
NMR

Infrared/Raman (~5%)

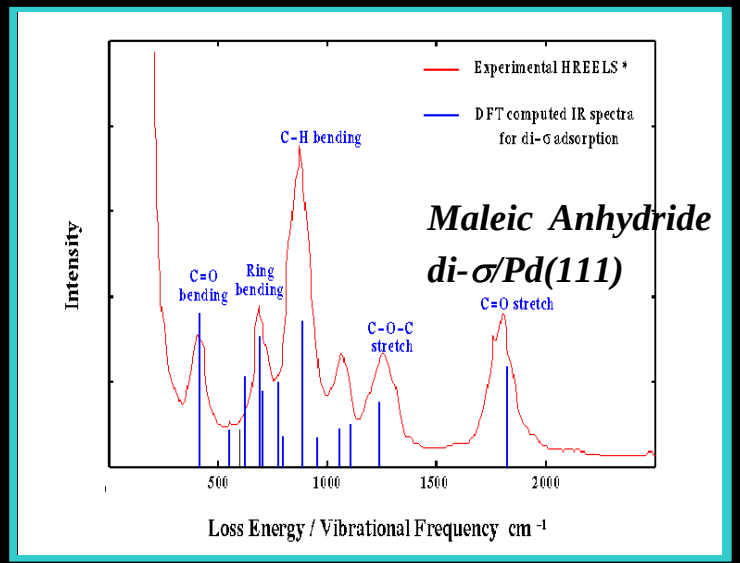

DFT–Predicted Adsorption Energies

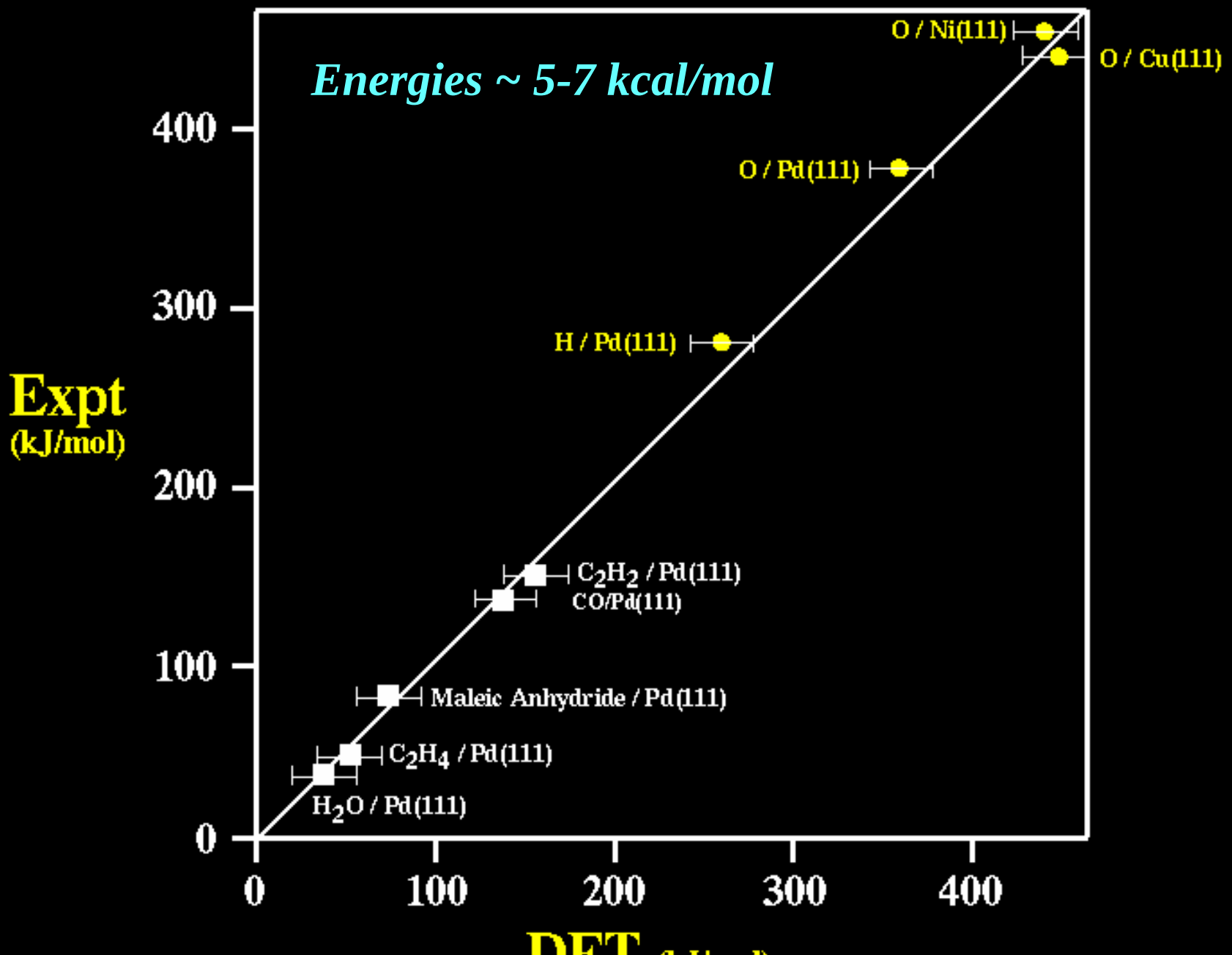

Quantum Mechanical Methods

Catalytic Reactivity

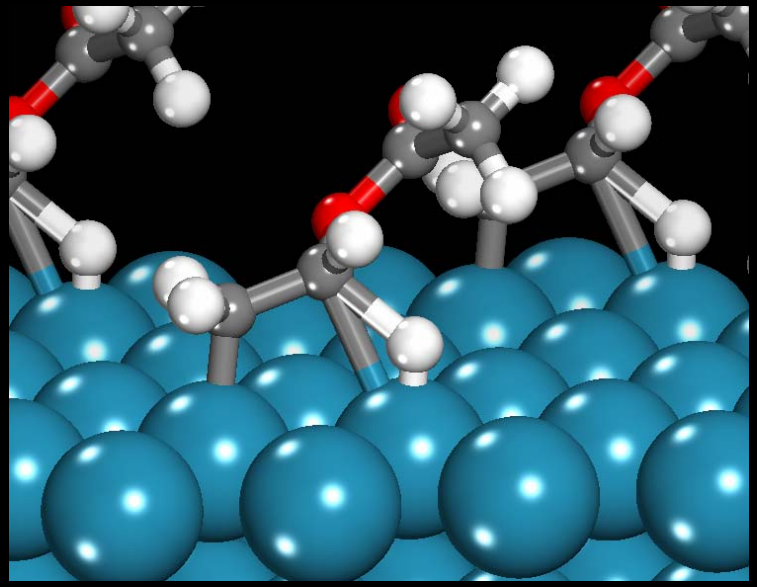

Semiempirical Methods
Density Functional Theory
Ab Initio Wave Function Methods
QM/MM (ONIOM model)
Ab initio Molecular Dynamics

Structure, Reactivity and Mechanisms

Method Accuracy is a Critical Issue

Model Accuracy is a Critical Issue

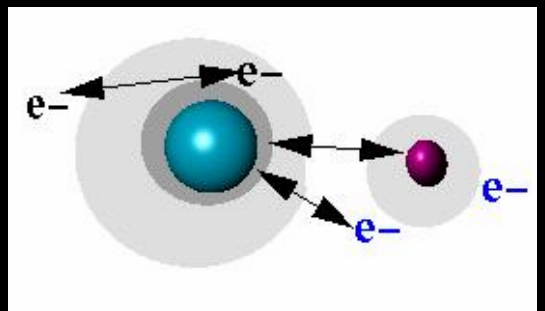

Catalytic Kinetics

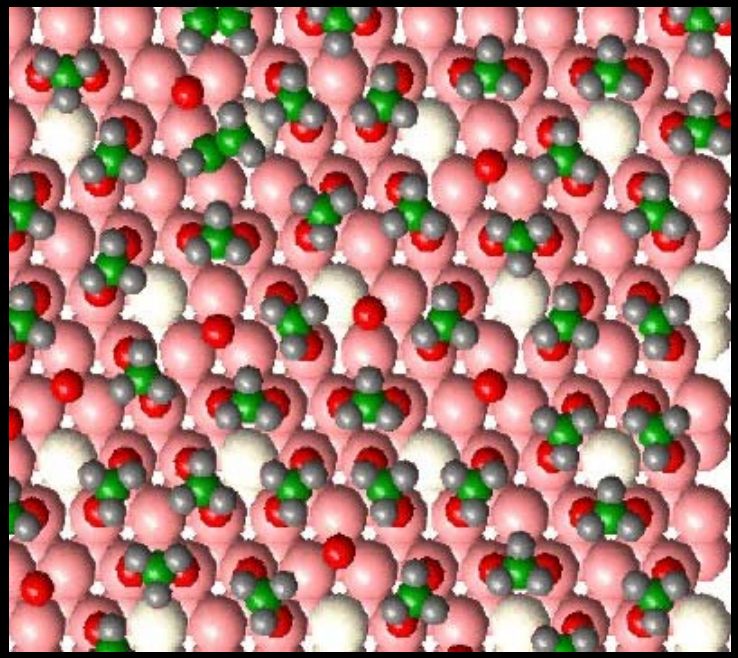

Lattice Gas Models

Kinetic Monte Carlo Simulations

Microkinetic Modeling

Reaction Kinetics for Various Systems

(TPD, steady state and transient kinetics)

Modeling Surface Reactivity

Quantum Chemistry

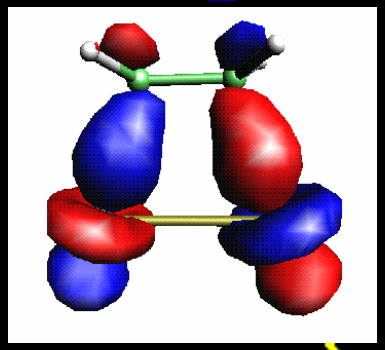

Reaction Mechanism
Adsorption Energies
Activation Barriers
Rate Constants
Equilibrium Constants

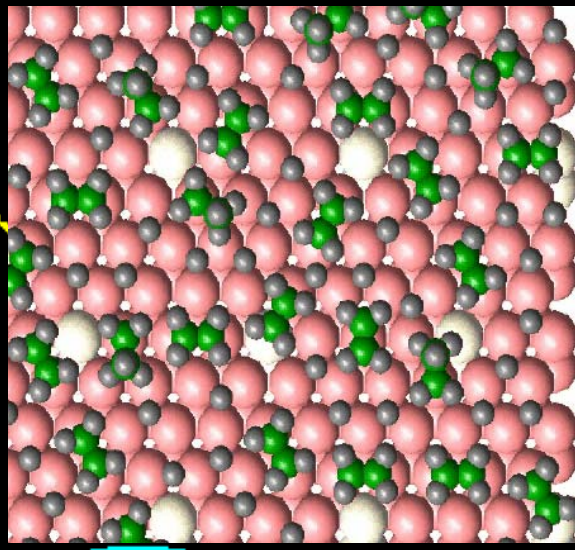

Reactivity

Monte Carlo Simulation

Kinetics Depend on Local Surface Structure

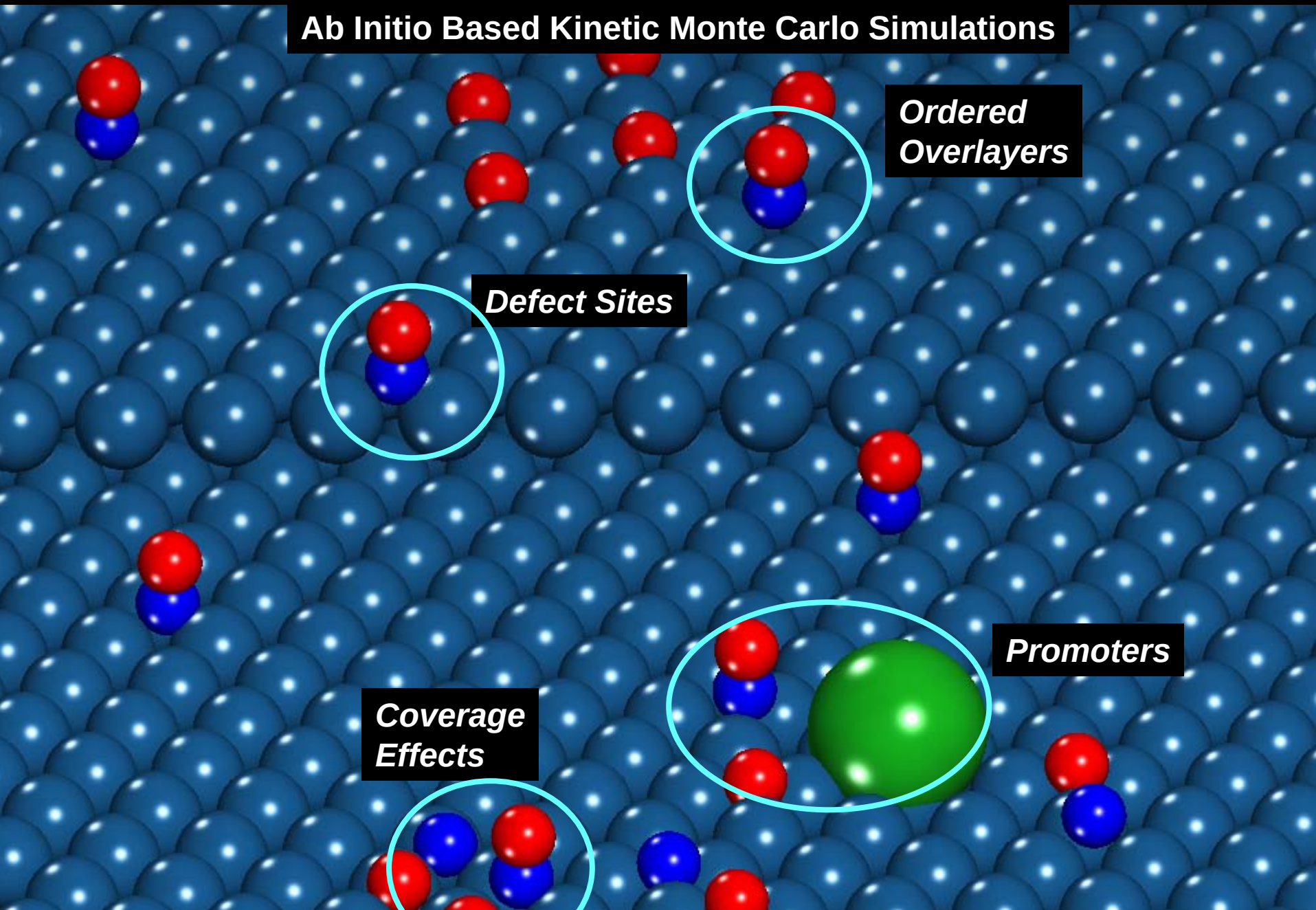

Motivating Example Systems

VAM Synthesis

Electrocatalytic Oxidation of Methanol

Vinyl Acetate Synthesis

Selective and Unselective Pathways

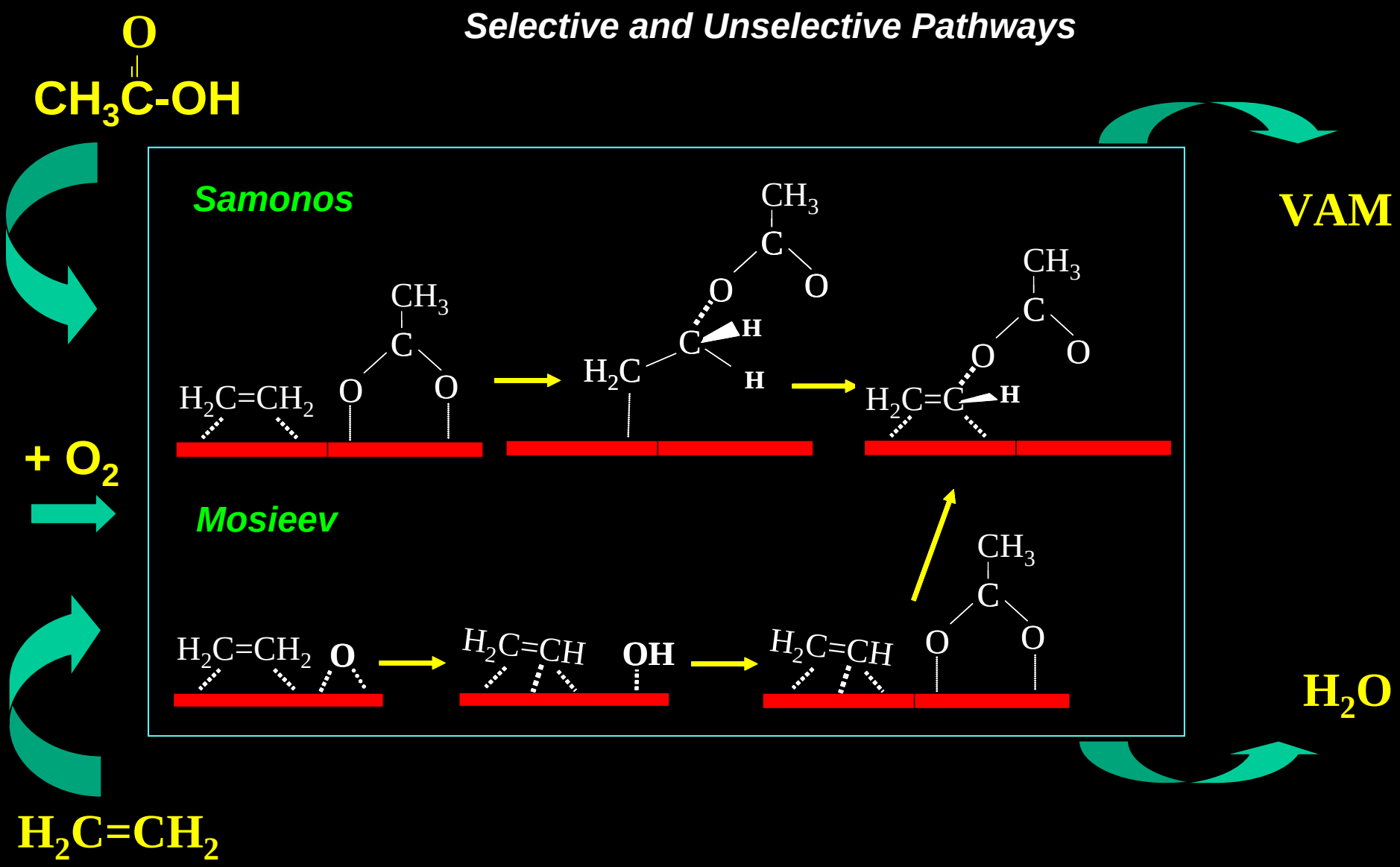

Critical Steps in Samonos Mechanism

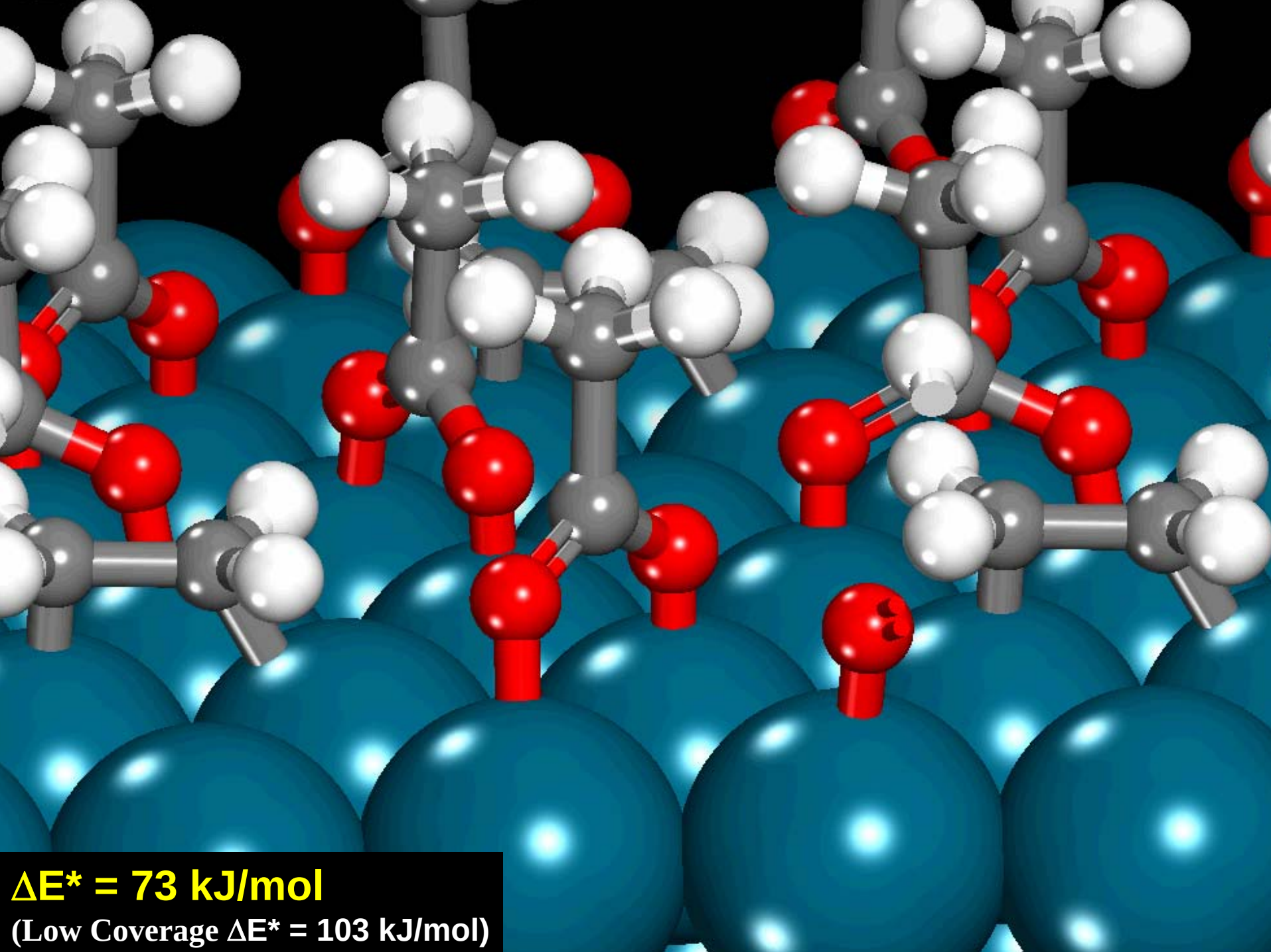
ΔE* = 73 kJ/mol
(Low Coverage ΔE* = 103 kJ/mol)

Transition State: β-Hydride Elimination - Acetoxyethyl

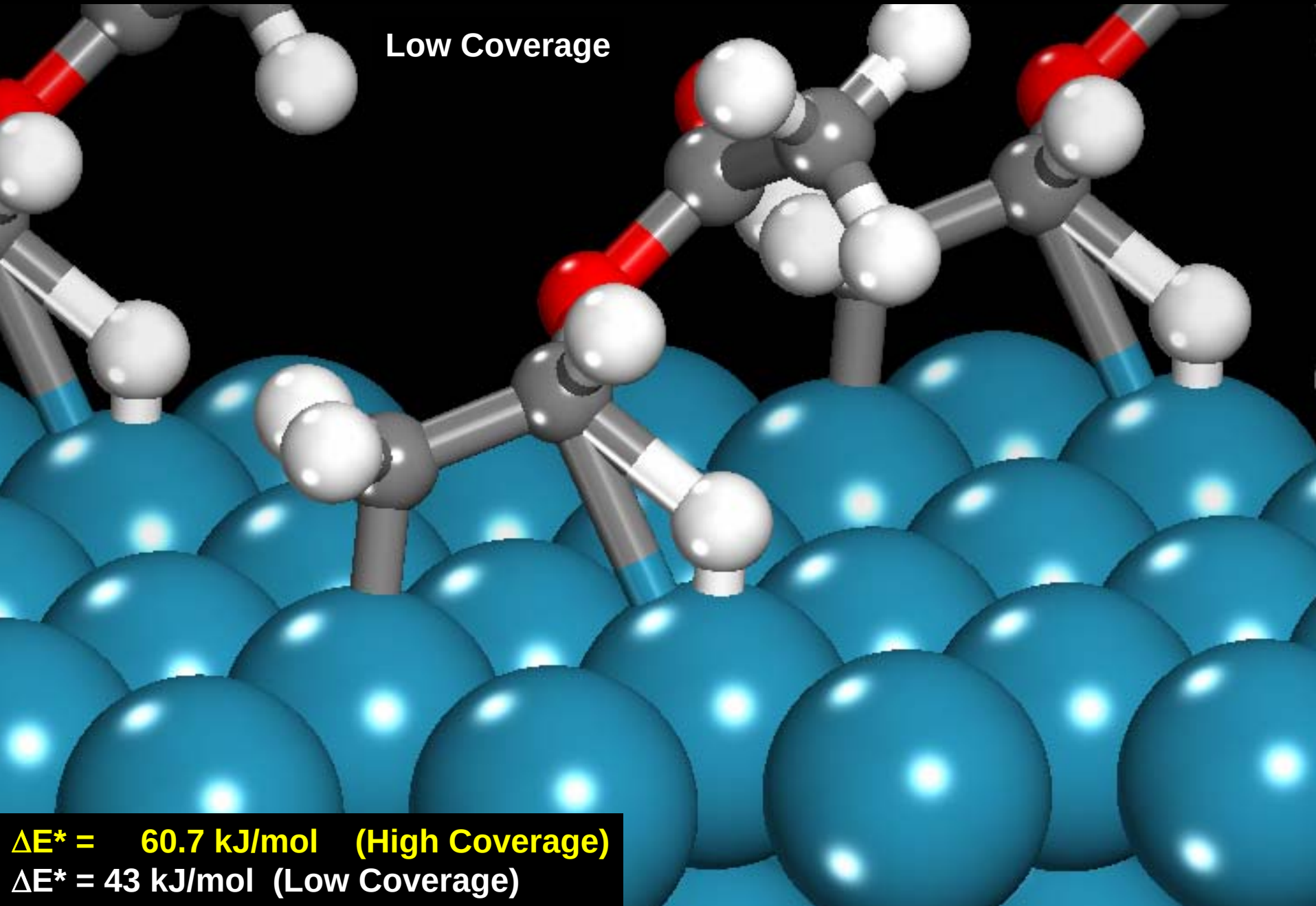

$\Delta E^* =$ 60.7 kJ/mol (High Coverage)

$\Delta E^* =$ 43 kJ/mol (Low Coverage)

Vinyl Acetate Synthesis

Selective and Unselective Pathways

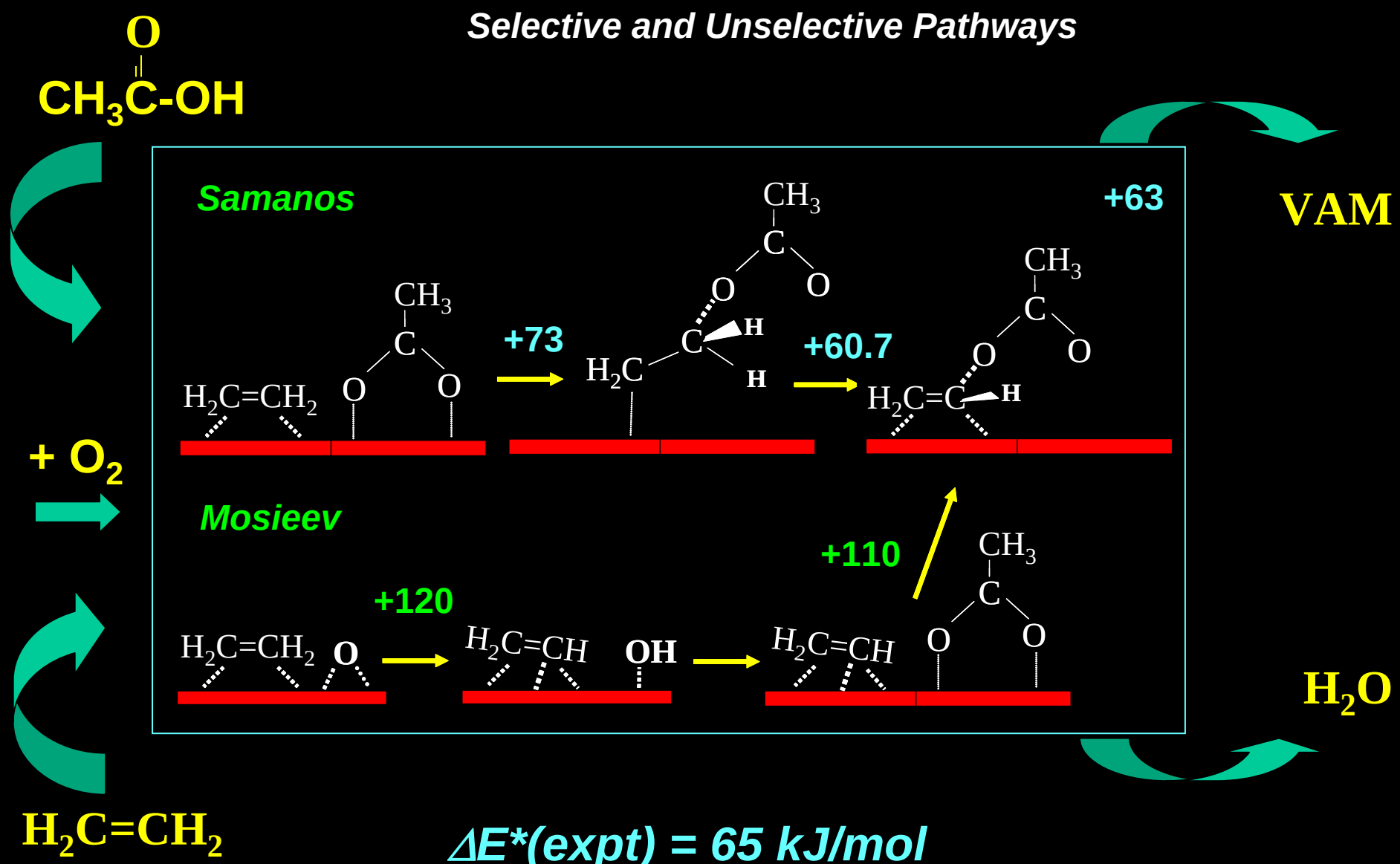

ΔE*(expt) = 65 kJ/mol

Formation of the Acetoxyethyl Intermediate

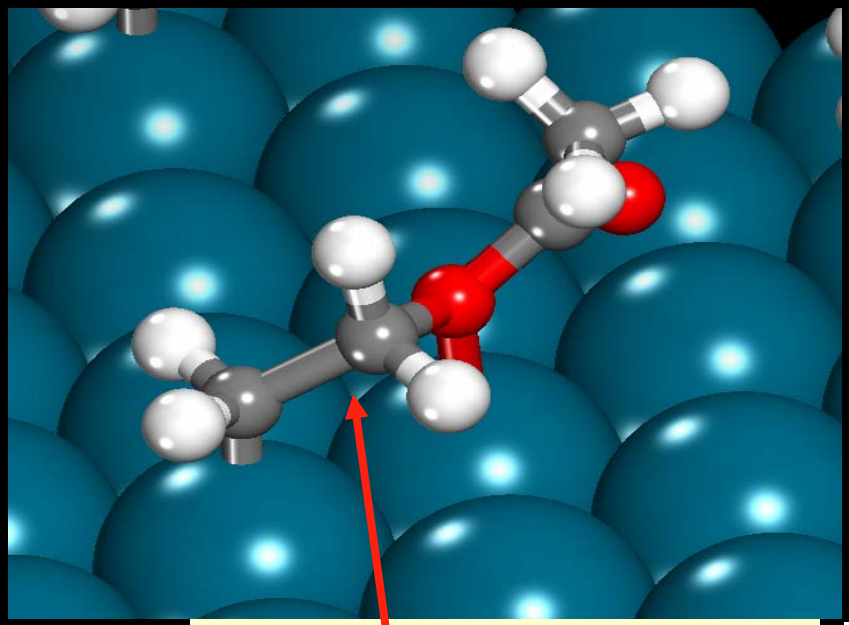

(1720)

Stacchiola, D., F. Calaza, L. Burkholder, A. Schwabacher, M. Neurock and W. T. Tysoe, Angew. Chemie Int. Ed., "44 (29) 4572-4574 2005.

(1778)

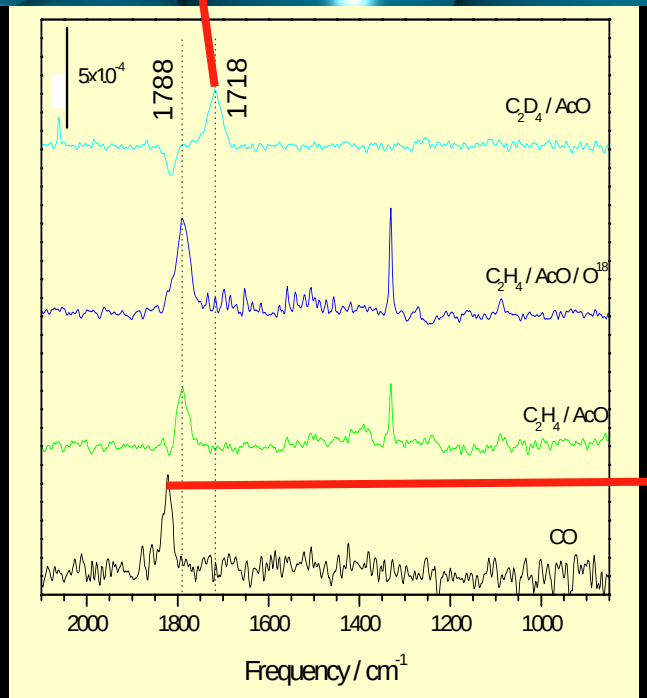

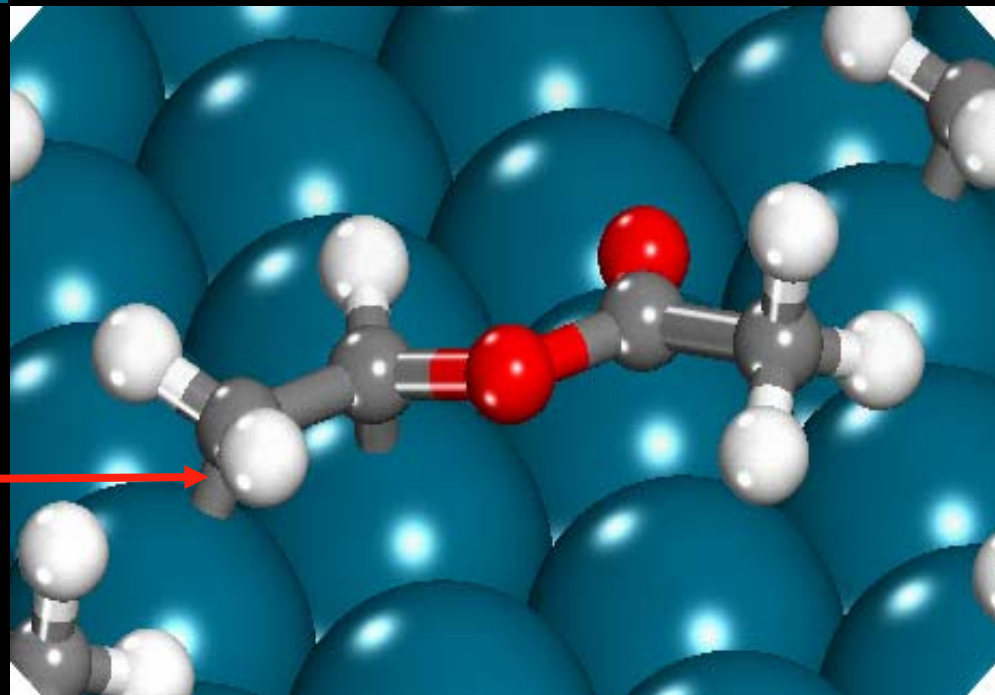

Reaction Kinetics

Vinyl Acetate Synthesis

	ν_{for}	ν_{rev}	E_{for}	E_{rev}
$O_2 = O^* + O^*$	1	10^{13}	0.0	42.4
$H_2 = H^* + H^*$	0.1	10^{13}	6.9	19.7
$C_2H_4 = C_2H_4^*$	1	10^{9}	0.0	14.0
$MeCO_2H = MeCO_2H^*$	1	10^{13}	0.0	11.9
$MeCO_2H = MeCO_2^* + H^*$	1	10^{13}	0.0	14.3
$MeCO_2H + O^* = MeCO_2^* + OH^*$	1	10^{13}	0.0	20.1
$CO = CO^*$	1	10^{13}	0.0	35.1
$CO_2 = CO_2^*$	1	10^{13}	0.0	5.6
$H_2O = H_2O^*$	1	10^{13}	0.0	9.6
$MeCO_2CHCH_2 = MeCO_2^* + CHCH_2^*$	1	10^{13}	5.6	15.8
$MeCO_2CHCH_2 + H^* = MeCO_2^* + CHCH_2^*$	1	10^{13}	0.	25.3
$C_2H_4 = CHCH_2^* + H^*$	1	10^{13}	8.1	7.0
$C_2H_4 + O^* = CHCH_2^* + OH^*$	1	10^{13}	3.6	8.3
$OH^* = O^* + H^*$	10^{13}	10^{13}	20.8	15.0
$2\,OH^* = O^* + H_2O^*$	10^{13}	10^{13}	5.6	19.4
$CH^* = C^* + H^*$	10^{13}	10^{13}	32.5	11.2
$CH^* + O^* = C^* + OH^*$	10^{13}	10^{13}	34.0	18.4
$CH_2^* = CH^* + H^*$	10^{13}	10^{13}	17.3	26.2

	ν_{for}	ν_{rev}	E_{for}	E_{rev}
$CH_2^* + O^* = CH^* + OH^*$	10^{13}	10^{13}	11.1	25.8
$C_2H_4^* + O^* = CHCH_2^* + OH^*$	10^{13}	10^{13}	17.7	8.3
$C_2H_4^* = CHCH_2^* + H^*$	10^{13}	10^{13}	22.1	7.0
$CHCH_2^* = CH^* + CH_2^*$	10^{13}	10^{13}	27.9	24.3
$CHCH_2^* = H^* + CCH_2^*$	10^{13}	10^{13}	24.6	16.3
$CHCH_2^* + O^* = OH^* + CCH_2^*$	10^{13}	10^{13}	18.8	16.2
$MeCO_2H^* = MeCO_2^* + H^*$	10^{13}	10^{13}	12.8	15.2
$MeCO_2H^* + O^* = MeCO_2^* + OH^*$	10^{13}	10^{13}	1.1	9.3
$MeCO_2^* + O^* = CH_2CO_2^* + OH^*$	10^{13}	10^{13}	18.7	12.1
$MeCO_2^* = CH_2CO_2^* + H^*$	10^{13}	10^{13}	23.9	11.5
$CH_2CO_2^* = CH_2 + CO_2^*$	10^{13}	10^{13}	6.3	0.0
$CHCH_3^* = CHCH_2^* + H^*$	10^{13}	10^{13}	15.7	13.3
$CHCH_3^* + O^* = CHCH_2^* + OH^*$	10^{13}	10^{13}	17.5	20.9
$CHCH_3^* = CCH_3^* + H^*$	10^{13}	10^{13}	14.8	29.6
$CHCH_3^* + O^* = CCH_3^* + OH^*$	10^{13}	10^{13}	8.5	29.1
$CCH_3^* = CCH_2^* + H^*$	10^{13}	10^{13}	33.2	7.7
$CCH_3^* + O^* = CCH_2^* + OH^*$	10^{13}	10^{13}	36.7	16.9
$CO^* = C^* + O^*$	10^{13}	10^{13}	70.6	0.0
$CCH_2^* = CH_2^* + C^*$	10^{13}	10^{13}	34.5	18.0
$CO_2^* = CO^* + O^*$	10^{13}	10^{13}	32.6	0.0

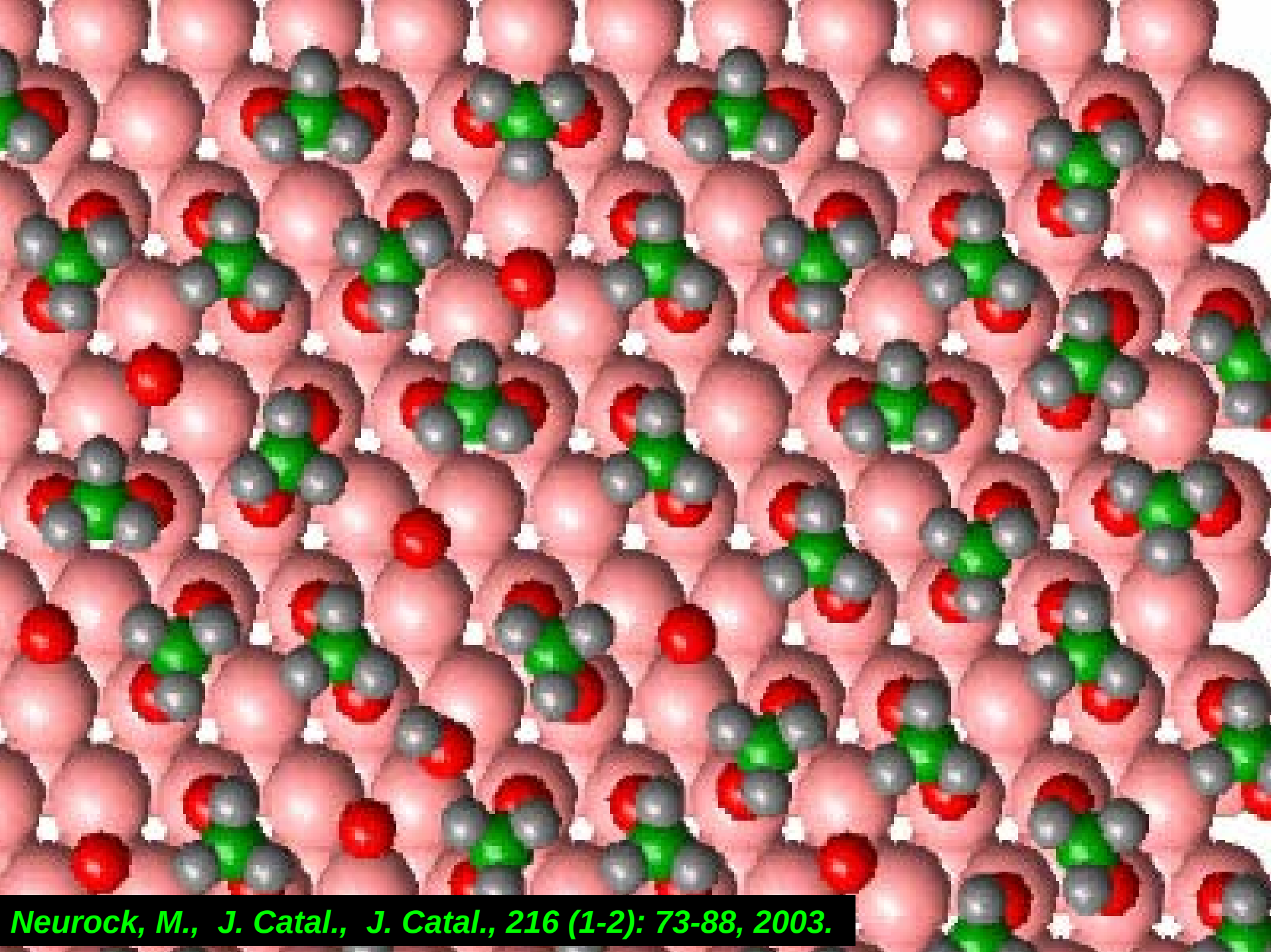

Neurock, M., J. Catal., J. Catal., 216 (1-2): 73-88, 2003.

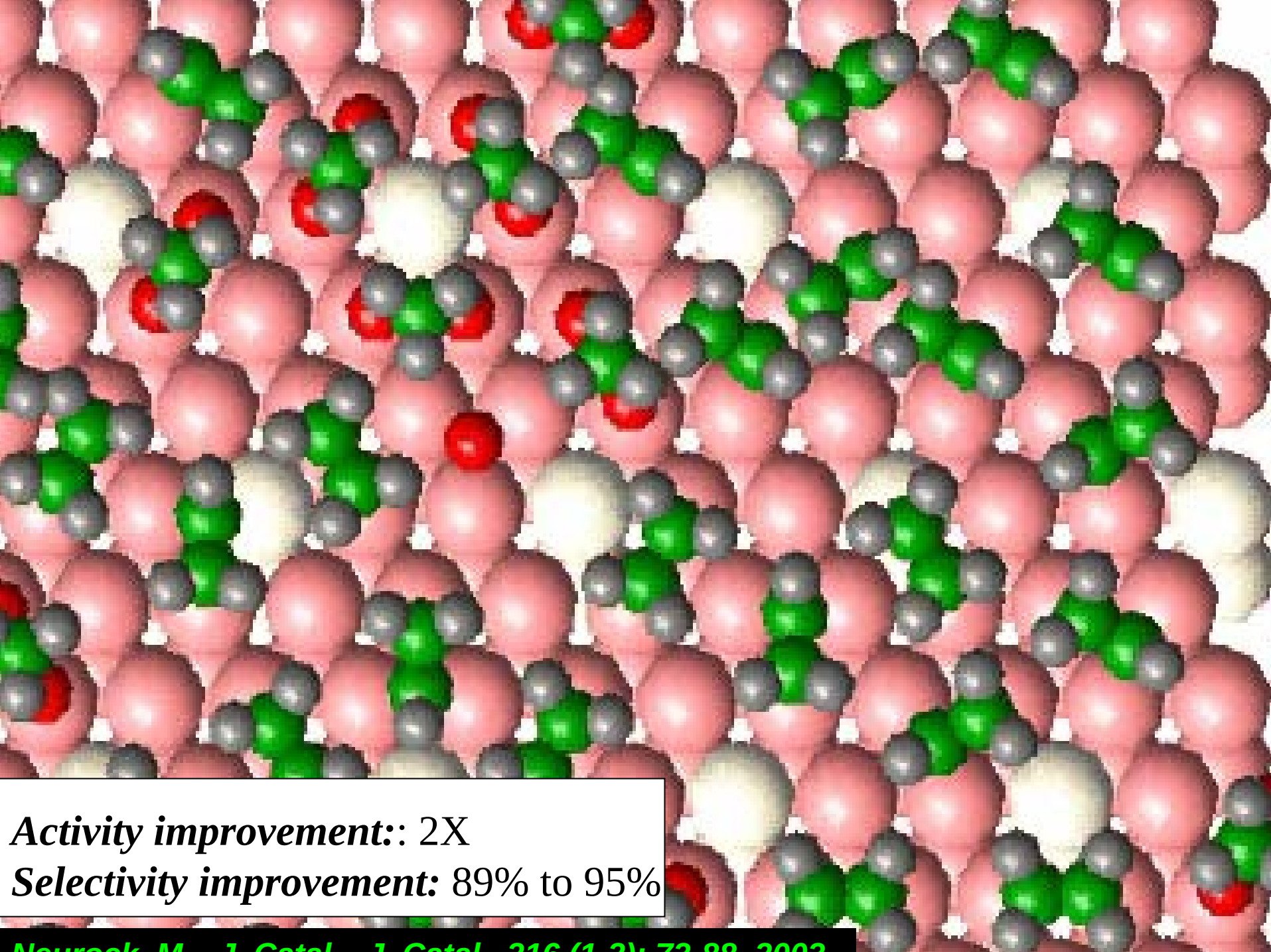

Activity improvement:: 2X
Selectivity improvement: 89% to 95%

Neurock, M., J. Catal., J. Catal., 216 (1-2): 72-88, 2003

VAM Summary

Au increases both activity and selectivity.

Au shuts down decomposition sites (Pd –ensembles) Improves selectivity.

Preferential surface patterning to enable "self-assembly" increases activity.

Results consistent with TAP experimental results from DuPont.

Conceptually consistent with results from Boudart for oxidation of hydrogen over Pd/Au particles.

Critical Issues

Can we synthesis specific ensembles?

Are these ensembles stable during reaction?

While these may be major limitations, approach suggests general features that can be engineering and opens up ideas for novel synthesis strategies.

Structures of Bimetallic Pd-Au Alloys

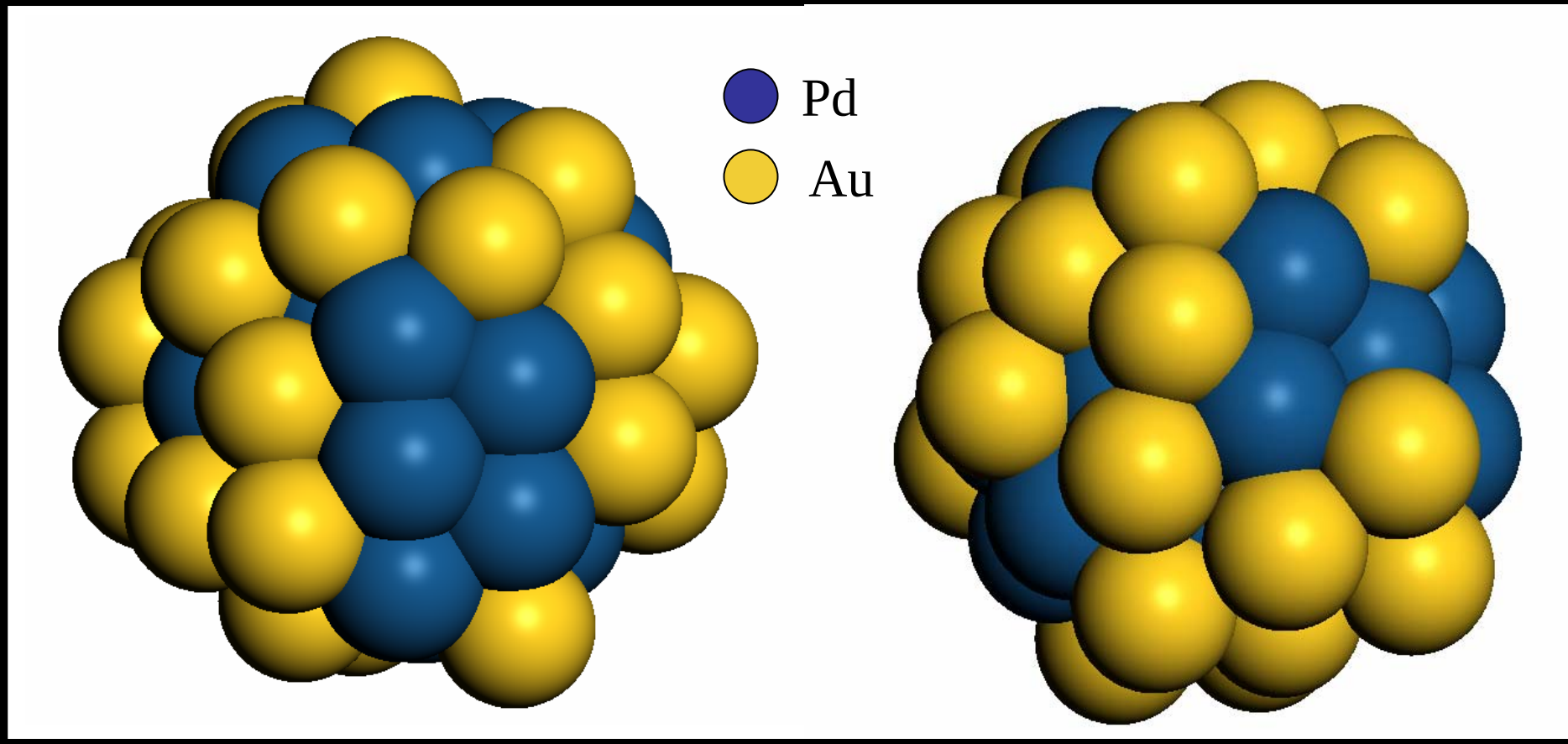

Amorphous or disordered structures were formed for Pd-Au clusters with these compositions

Direct Methanol Fuel Cell

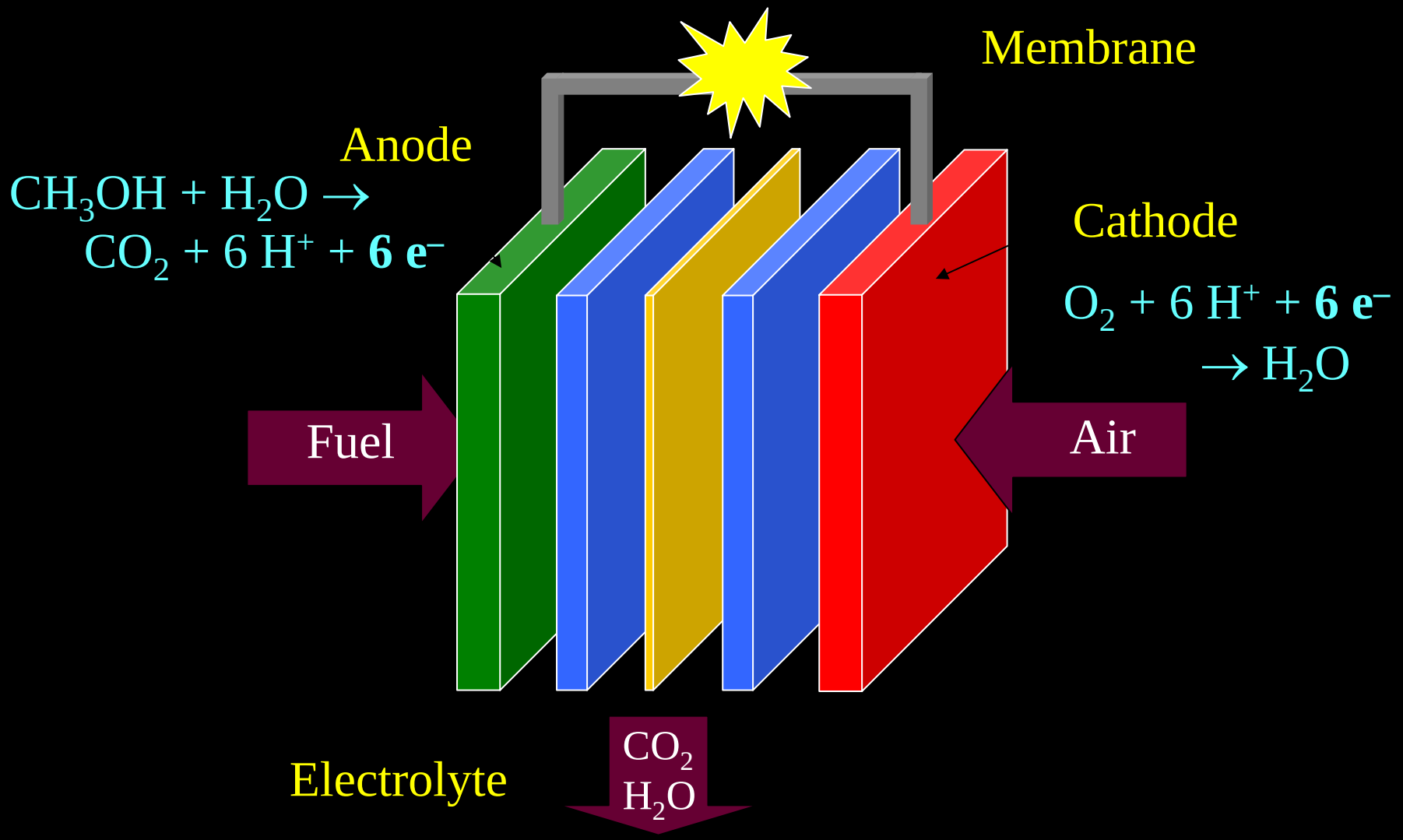

Complex Chemical Environment

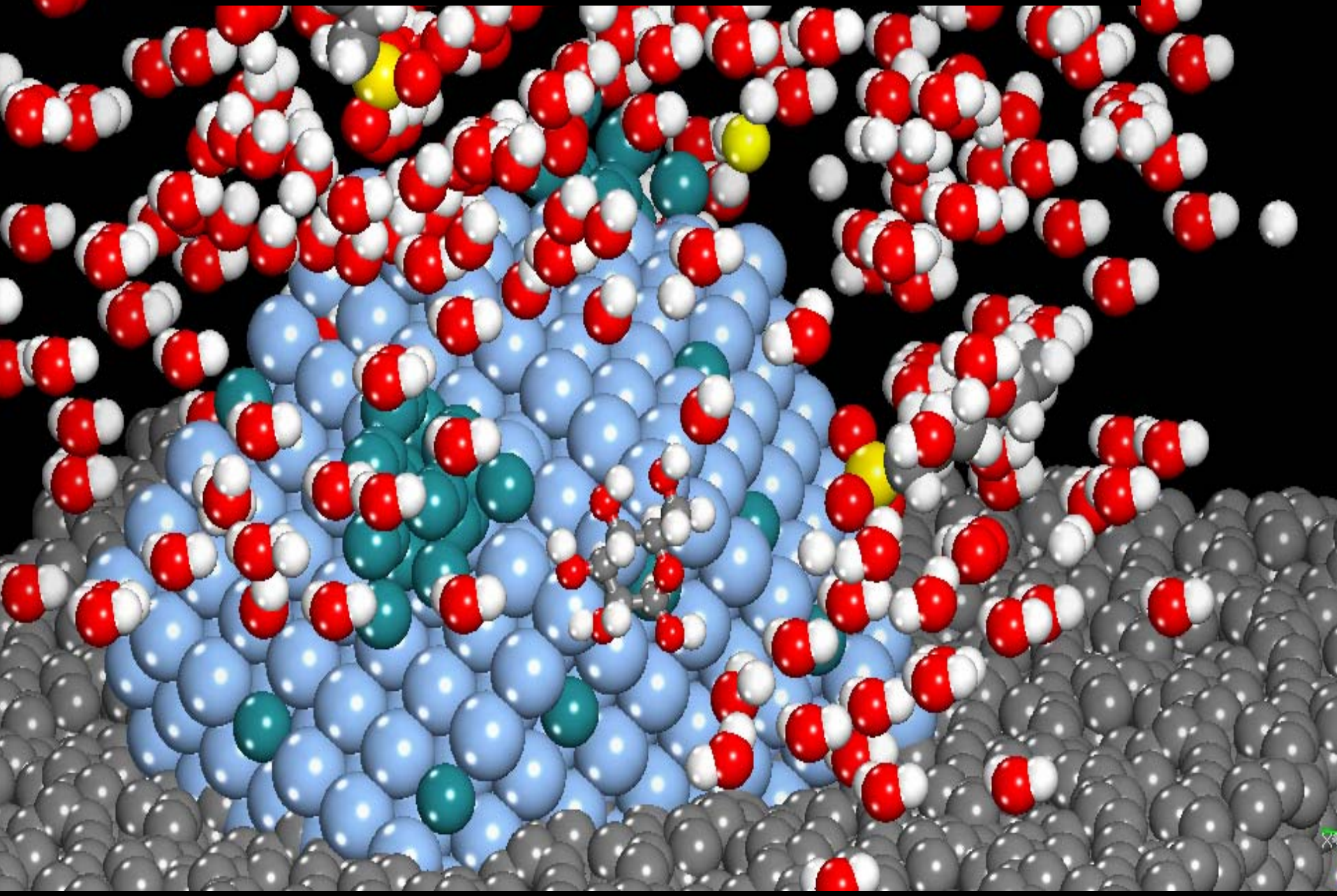

Disconnect Between QM and Electrochemisty

Isolated Capacitor

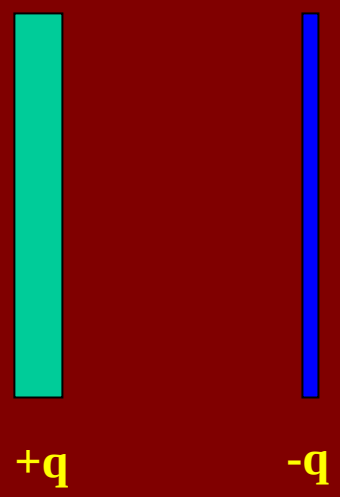

Ne = Constant

Canonical

F(T,V, Ne)

?

Constant Potential

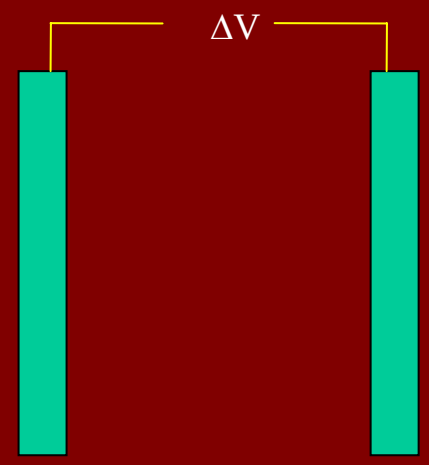

μ = Constant

Grand Canonical

μ(T,V, Ne)

Reactions lead to change in potential but the overall charge is the same.

Requires a new formalism

The Electrochemical Interface

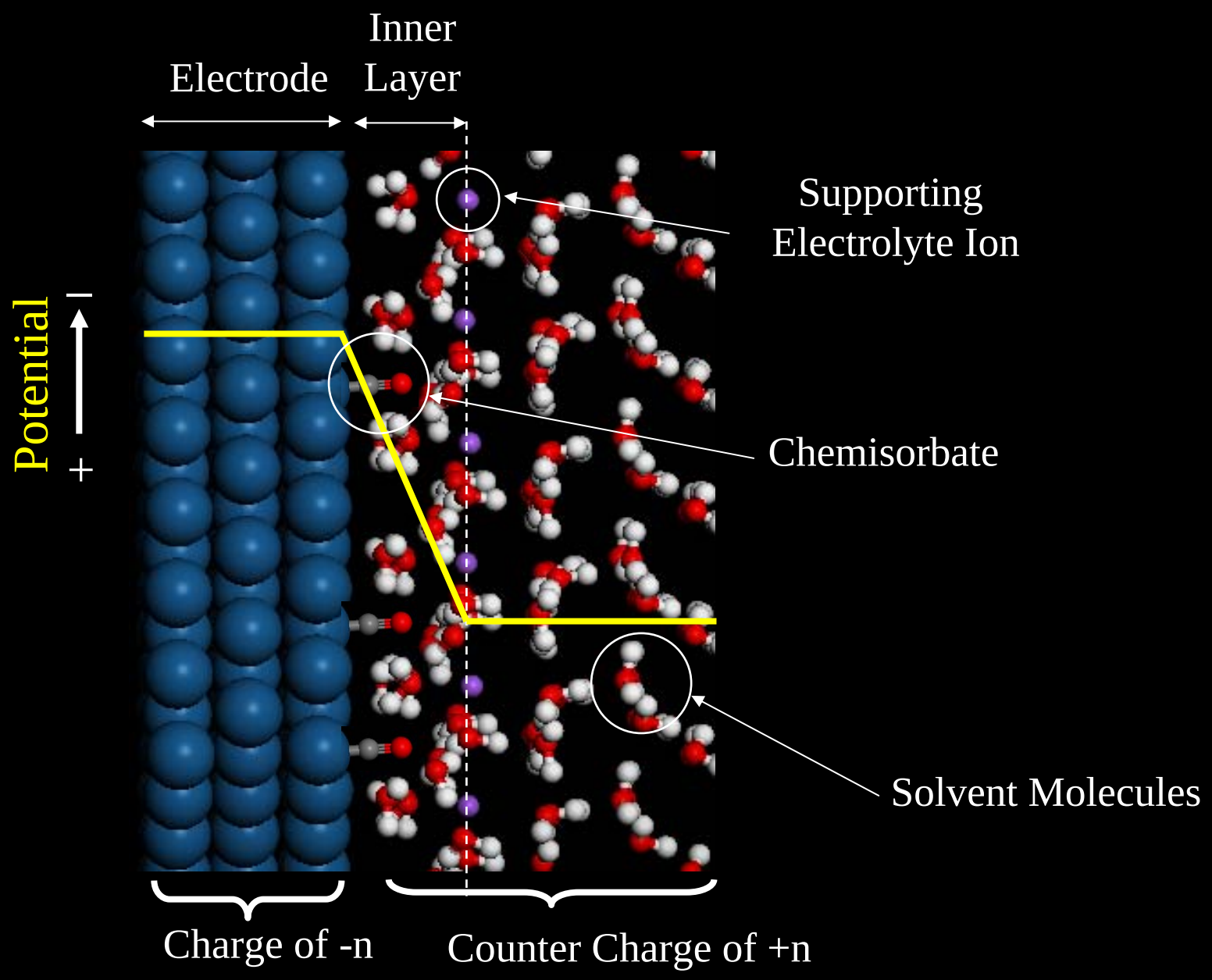

Approach

- Apply a charge to the metal.
- Establish the lowest energy structures for a particular charge.
- Determine the potential for this system.

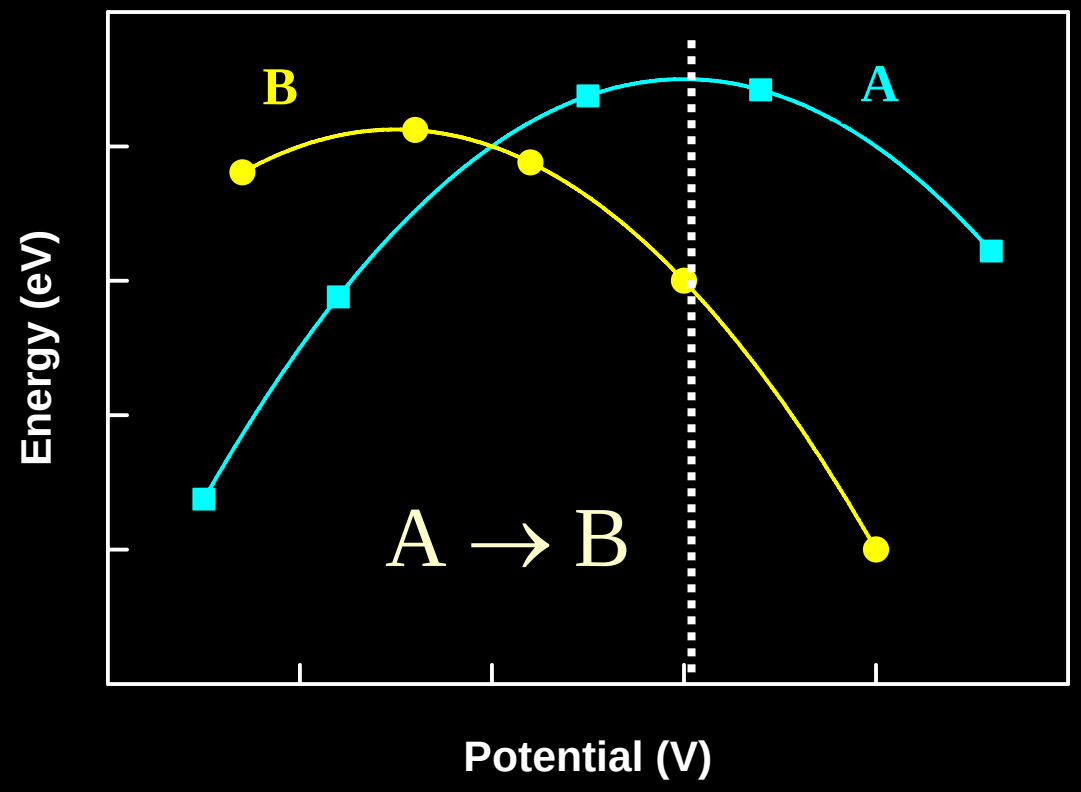

Water on Cu(111)

C. Taylor and M. Neurock, 2005

Cathodic Activation of Water

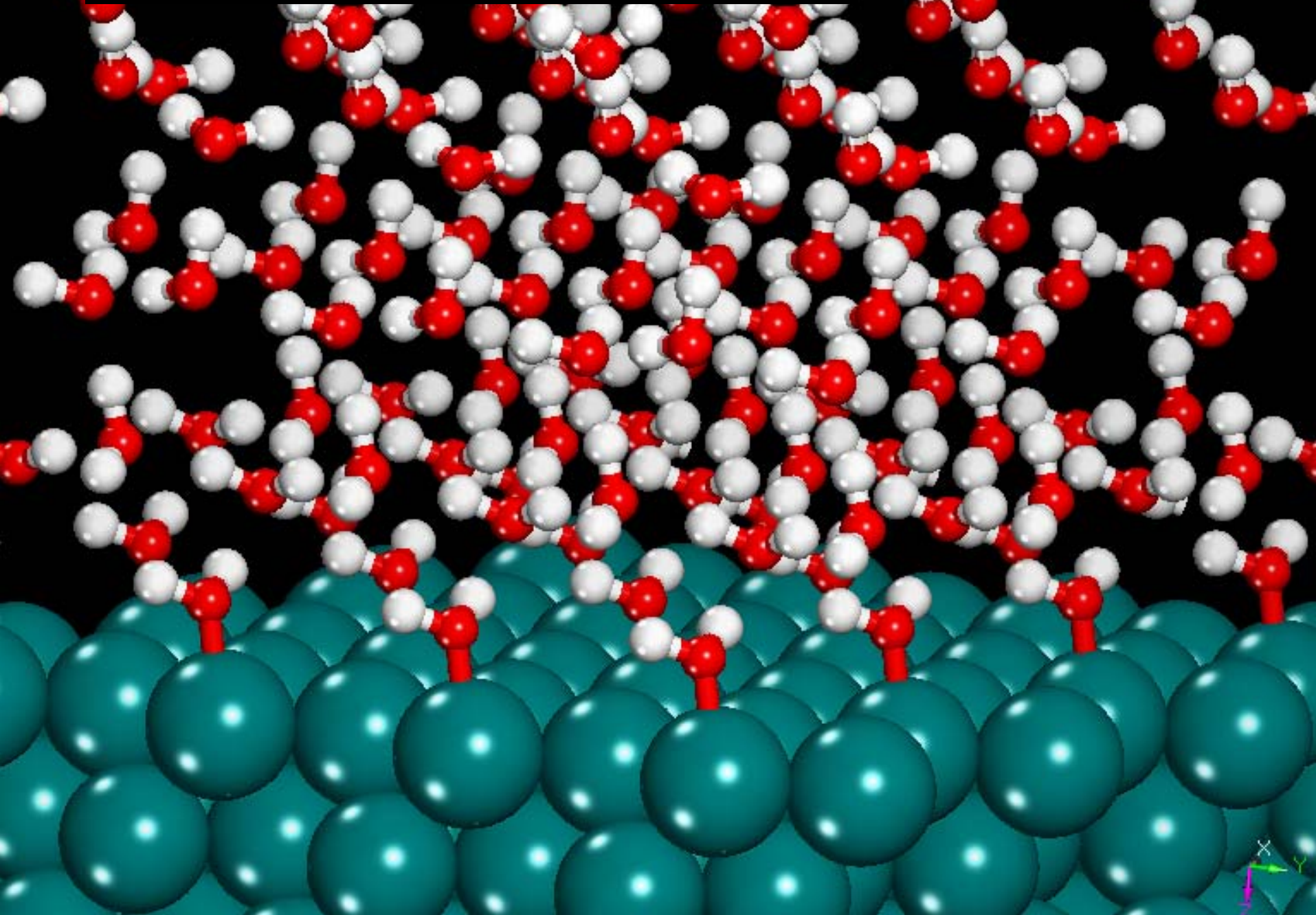

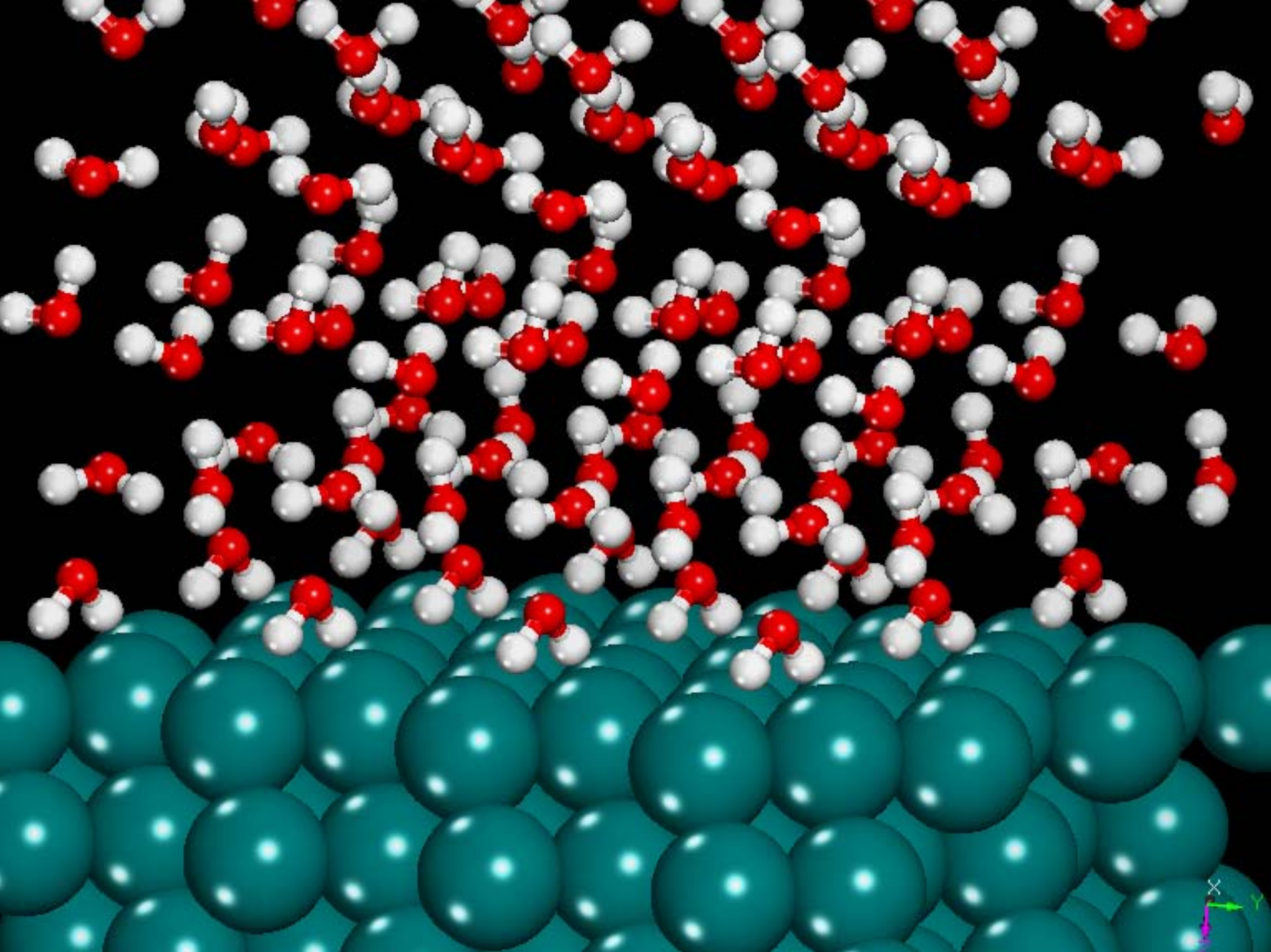
X
Y

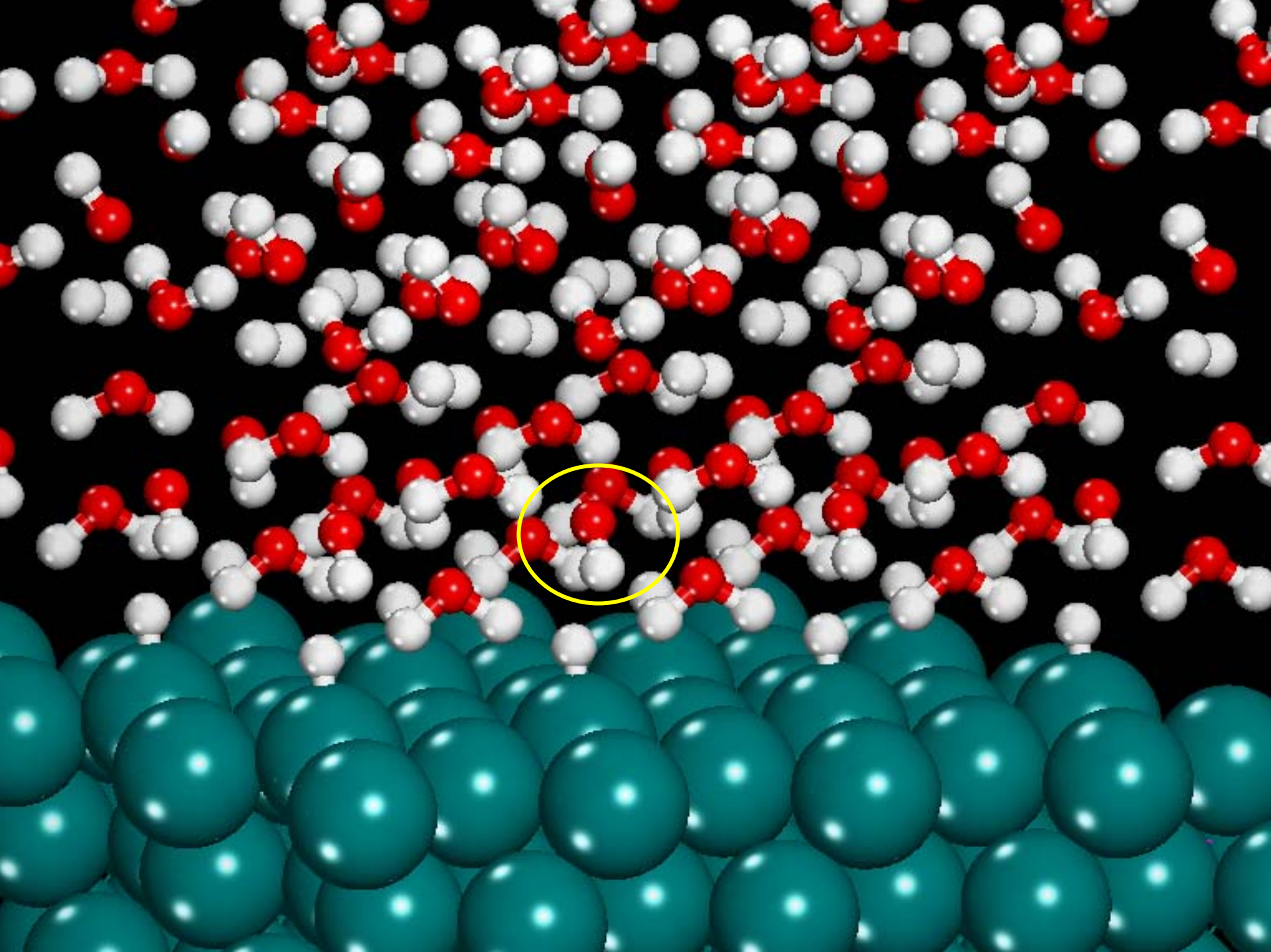

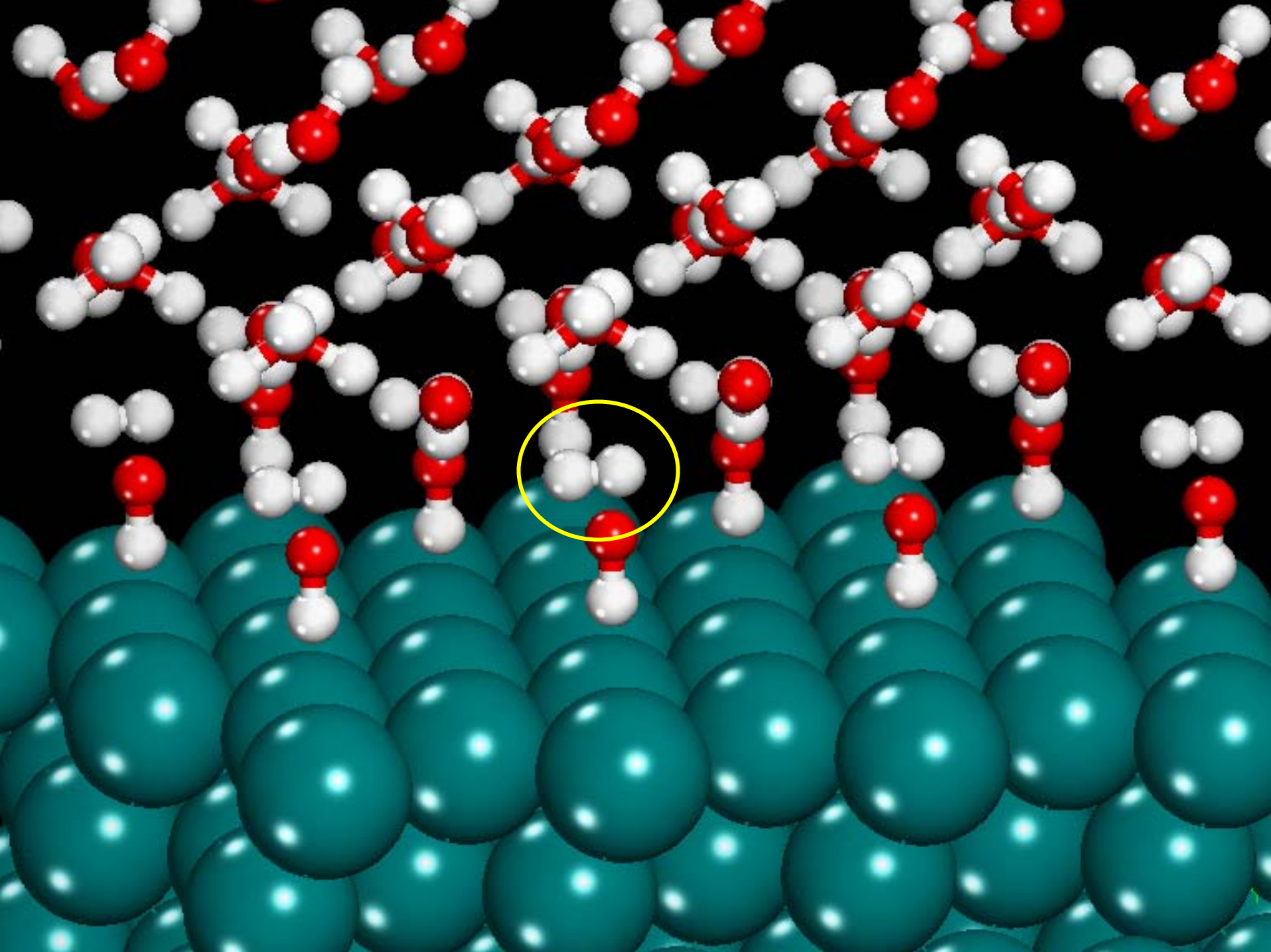

Anodic Activation of Water

(More positive potentials)

C. Taylor and M. Neurock, 2005

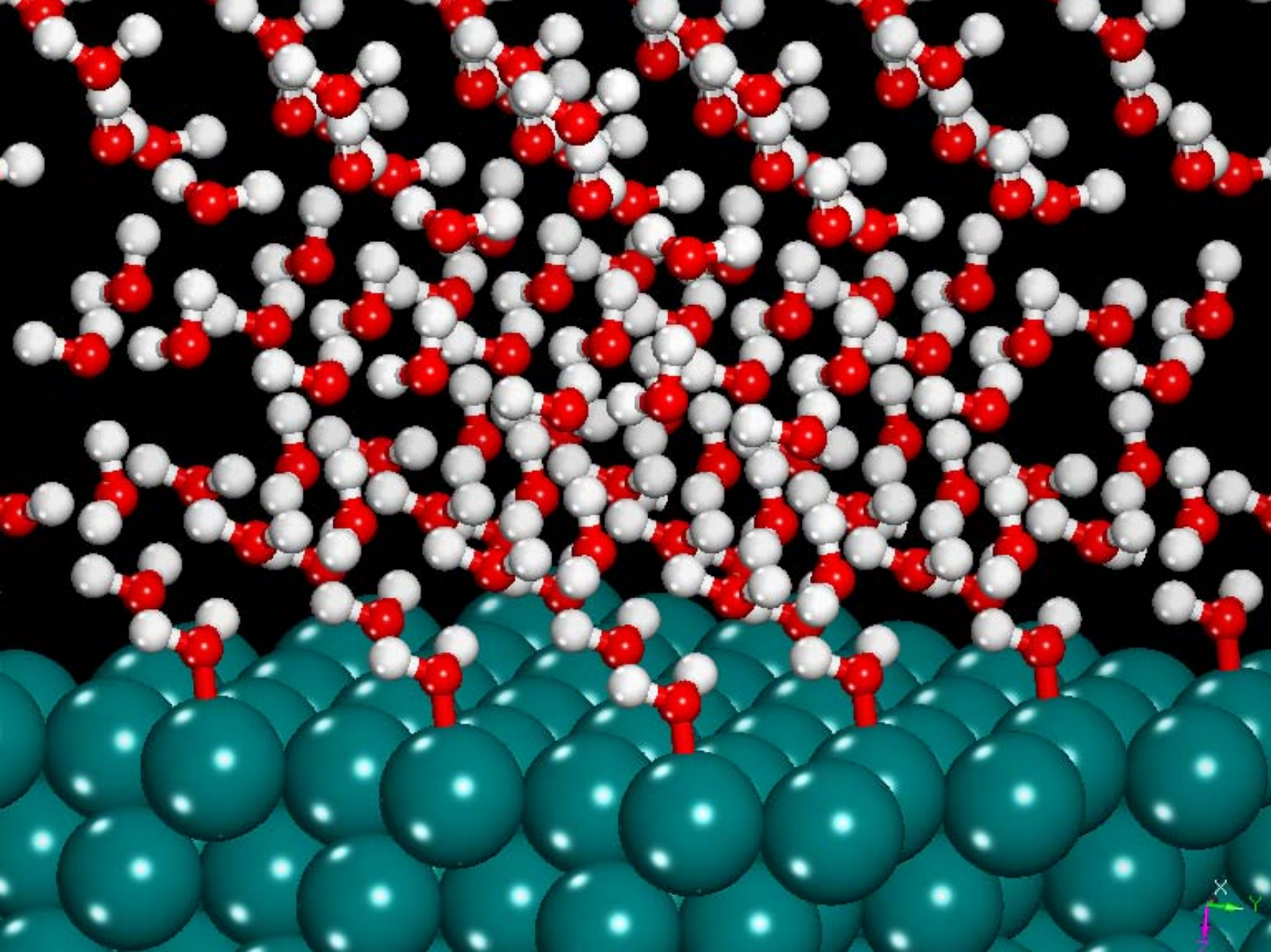
X
Y

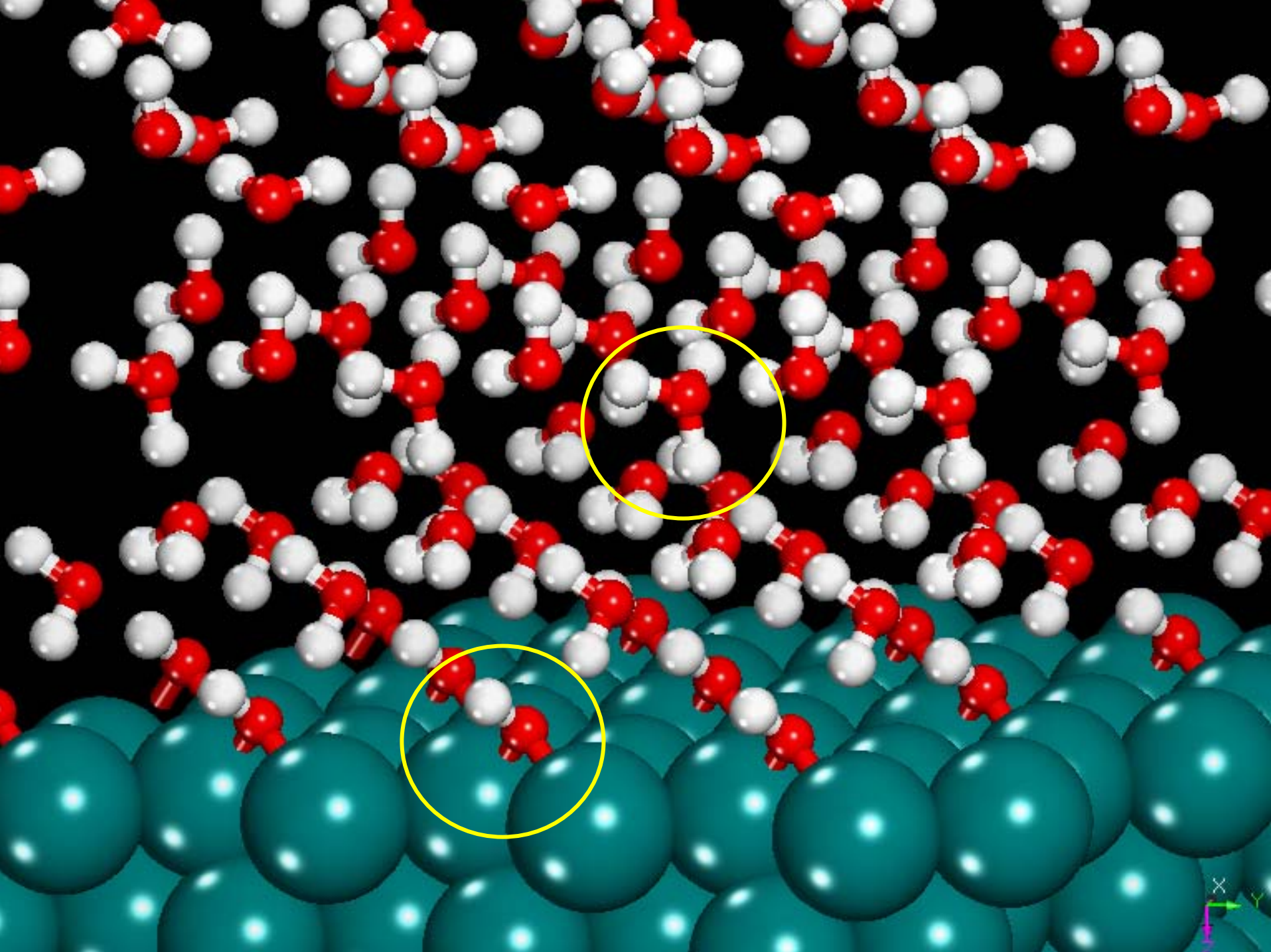
X
Y

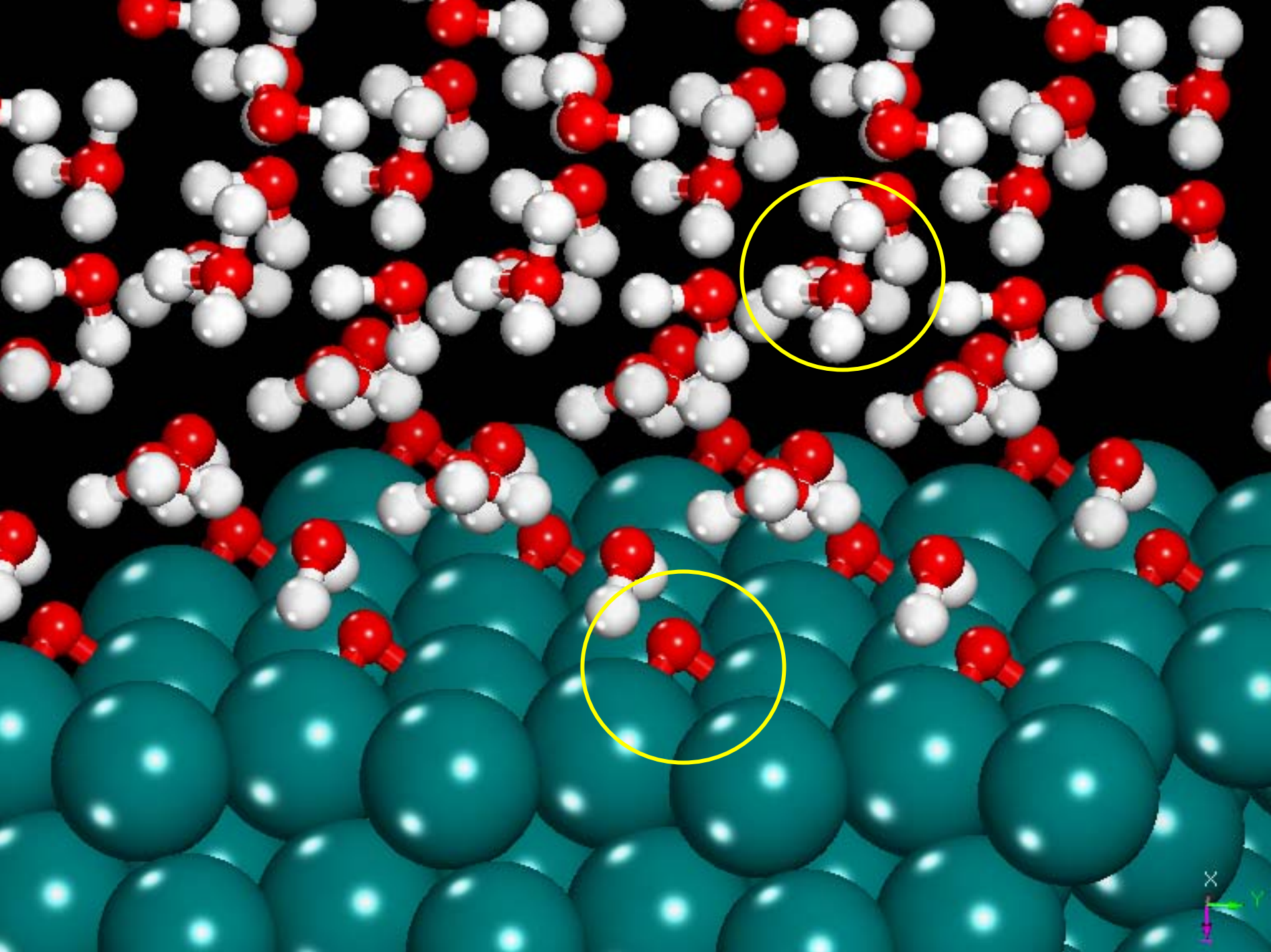
X
Y

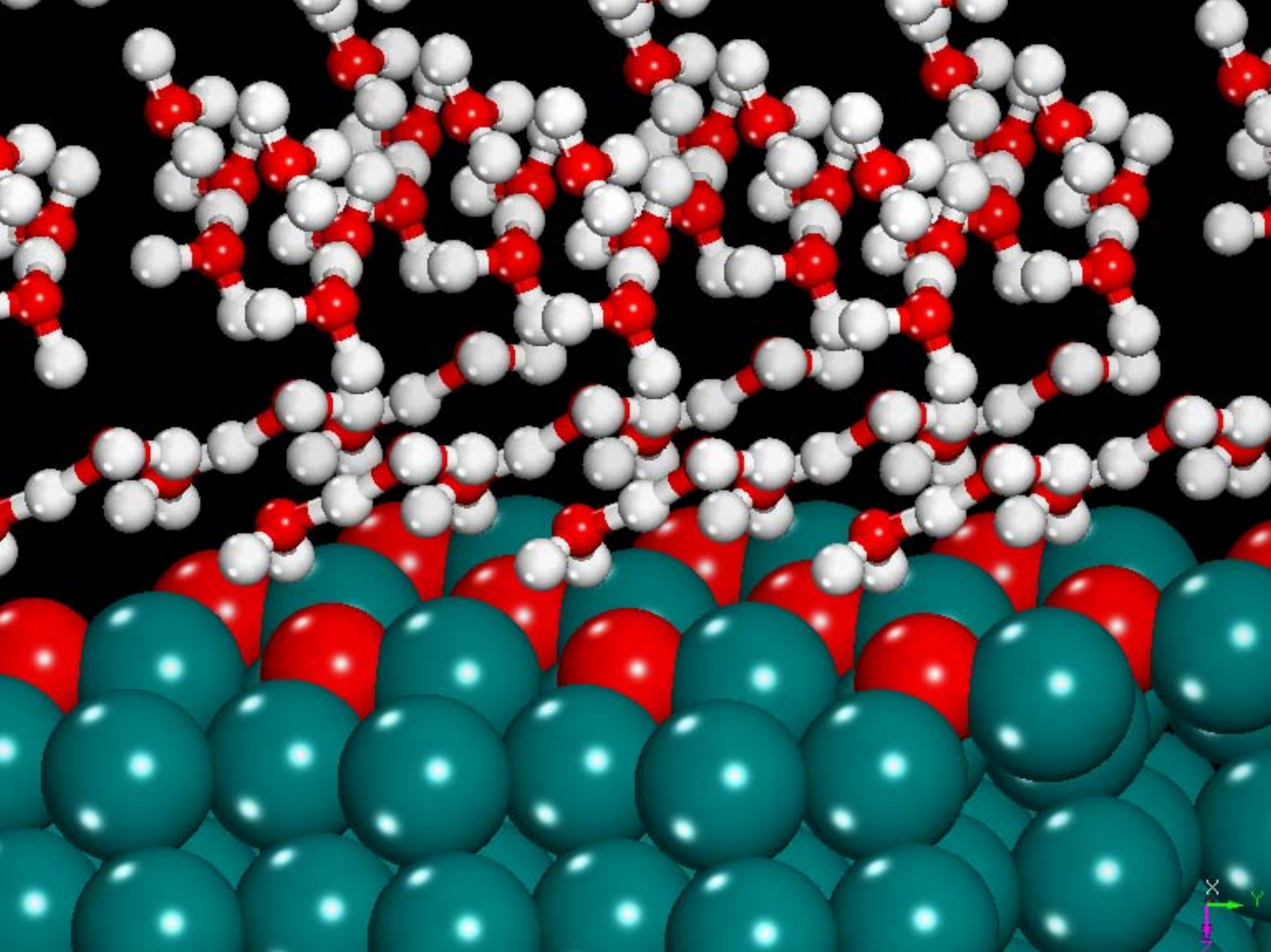
X
Y

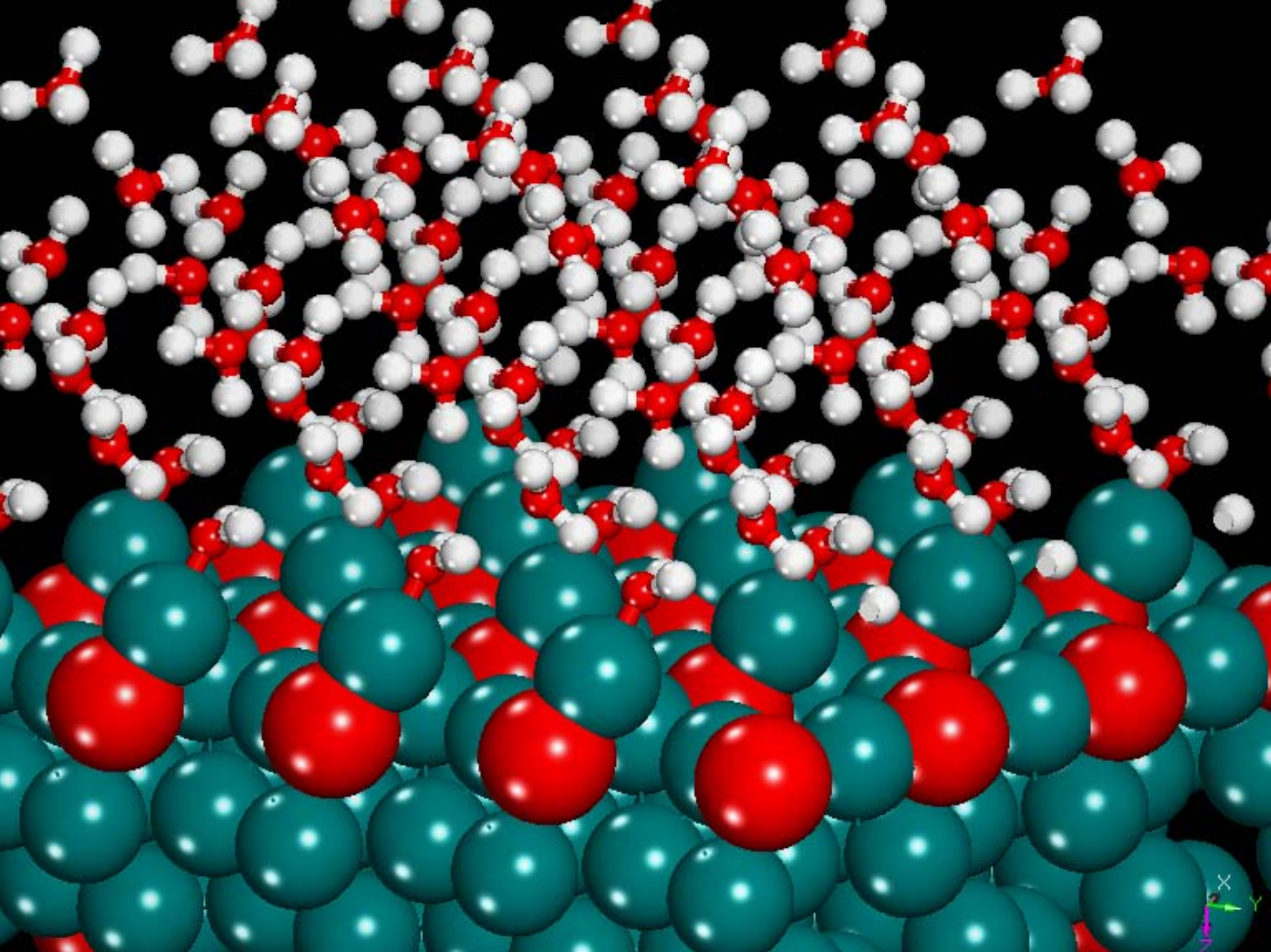
X
Y

Effects of Applied Potential on the H_2O/Pd Phase Diagram

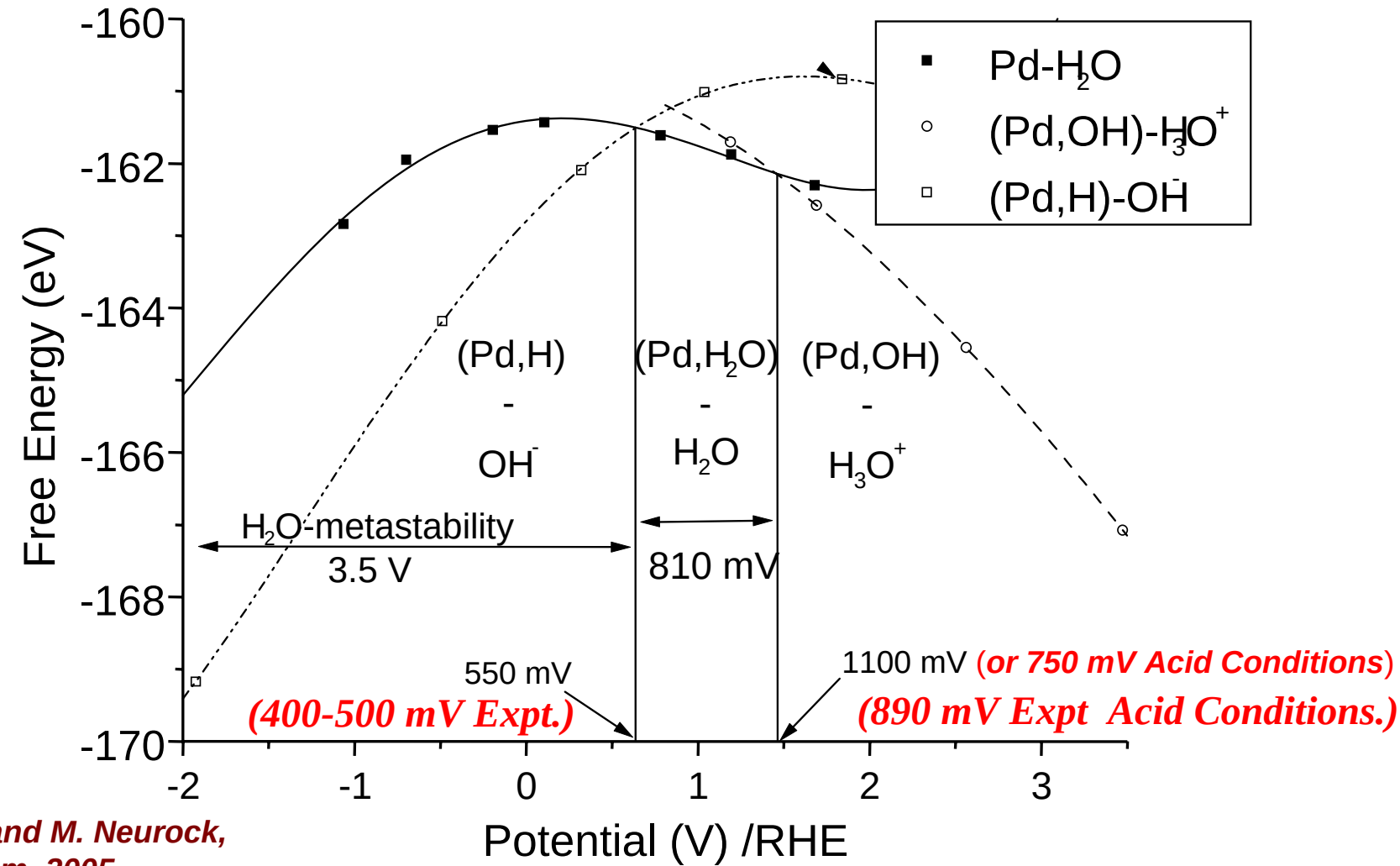

J.S. Filhol, and M. Neurock, Angew. Chem. 2005

Multidimensional Phase Diagram

Water/Ni

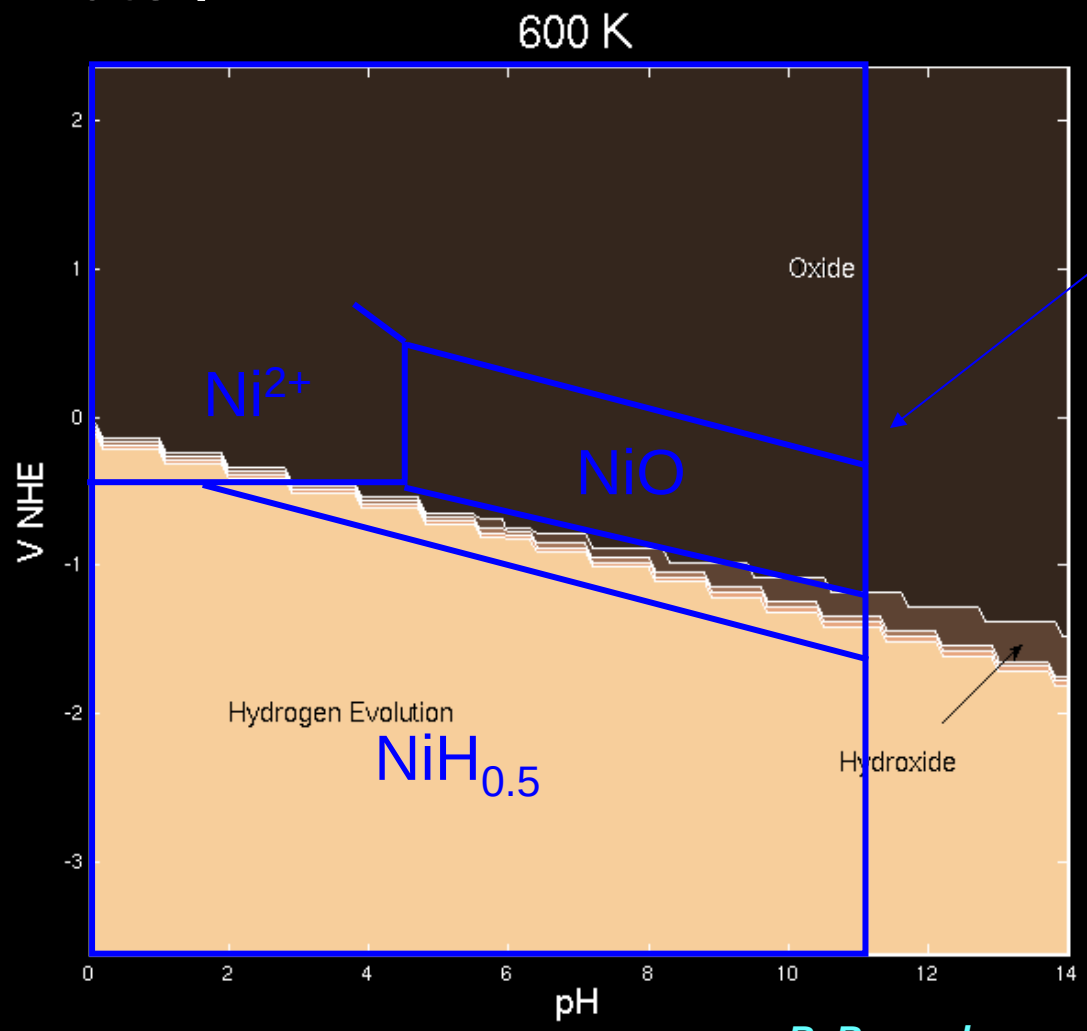

Beverskog and Puigdomenech

B. Beverskog and I. Puigdomenech. Corrosion Science 39 969 (1997)

Taylor, C. D., R.G. Kelly, and M. Neurock,, *J. Electrochem. Soc.*, 153, 2 , E207-E214, 2006.

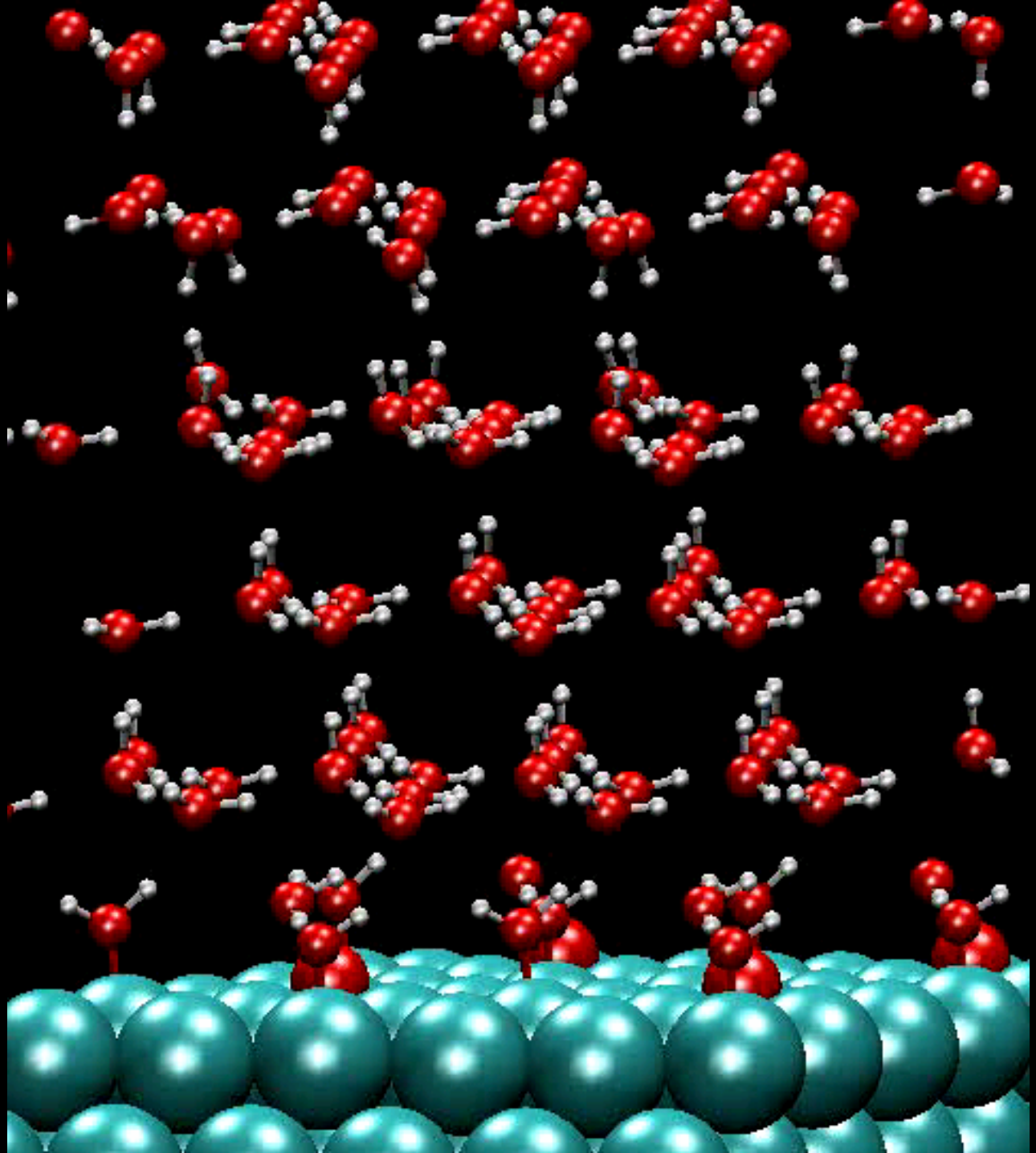

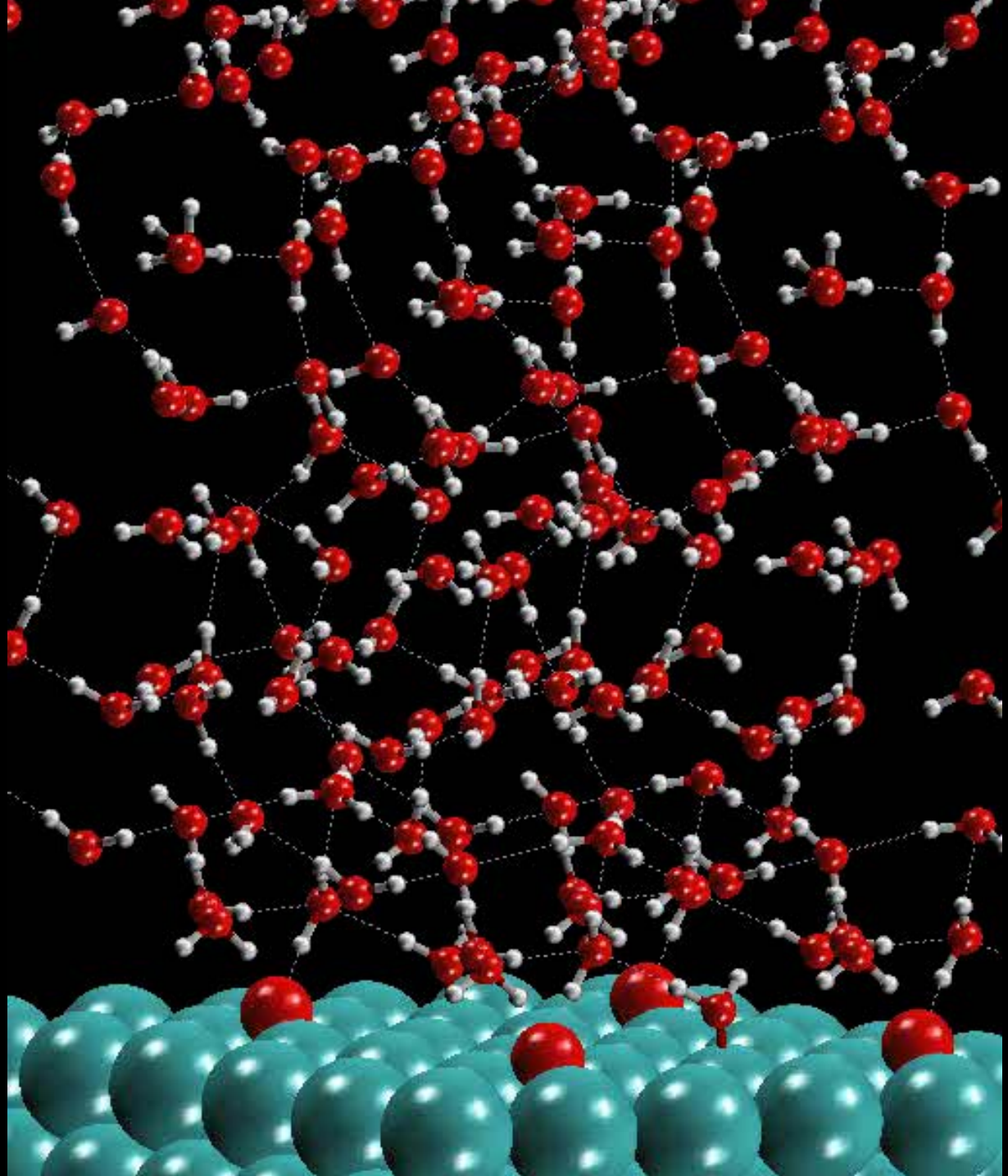

Electrocataltyic Oxidation of Methanol

Dual Path Mechanism

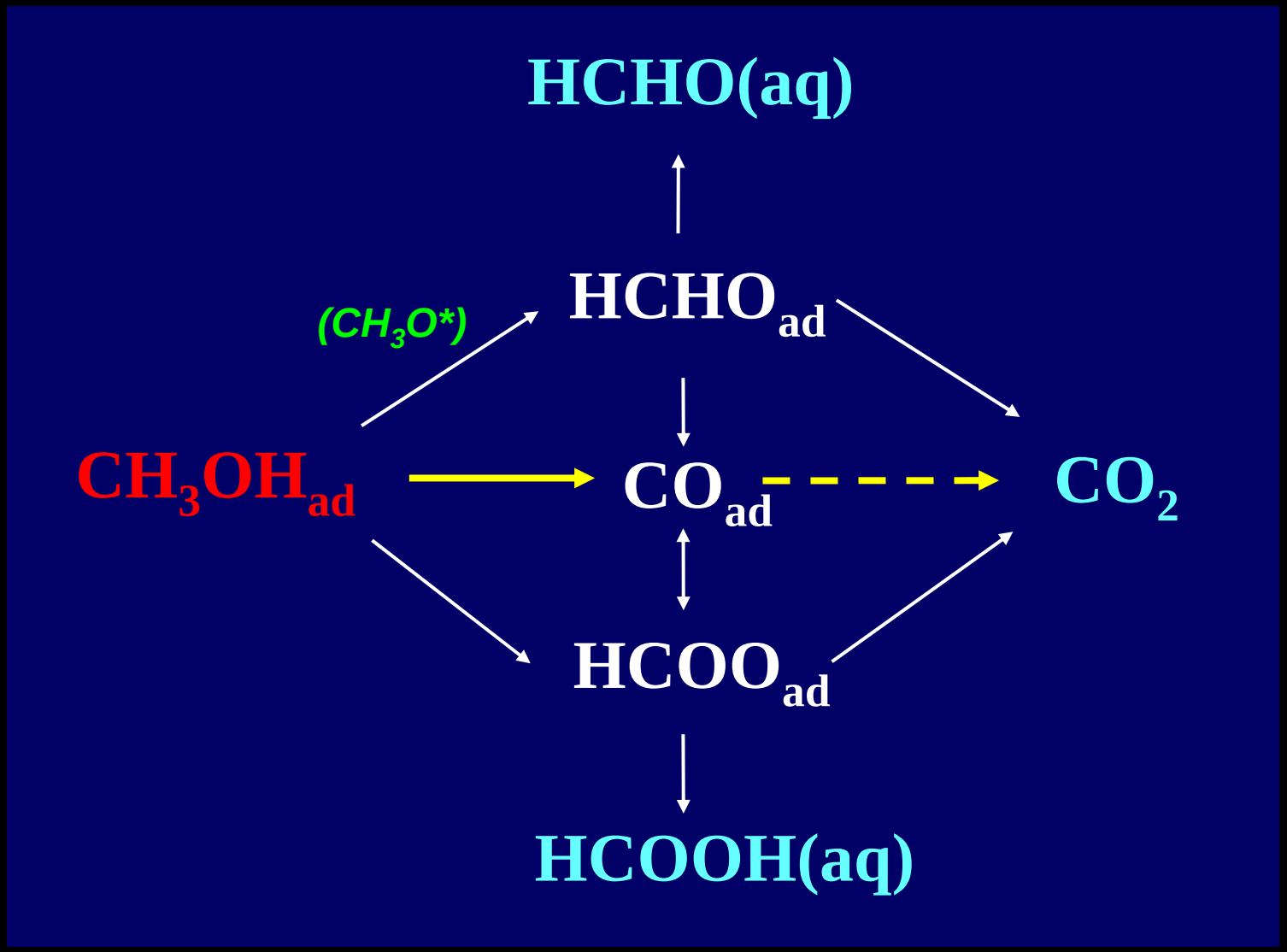

Methanol Dehydrogenation in the Aqueous Phase over Pt(111)

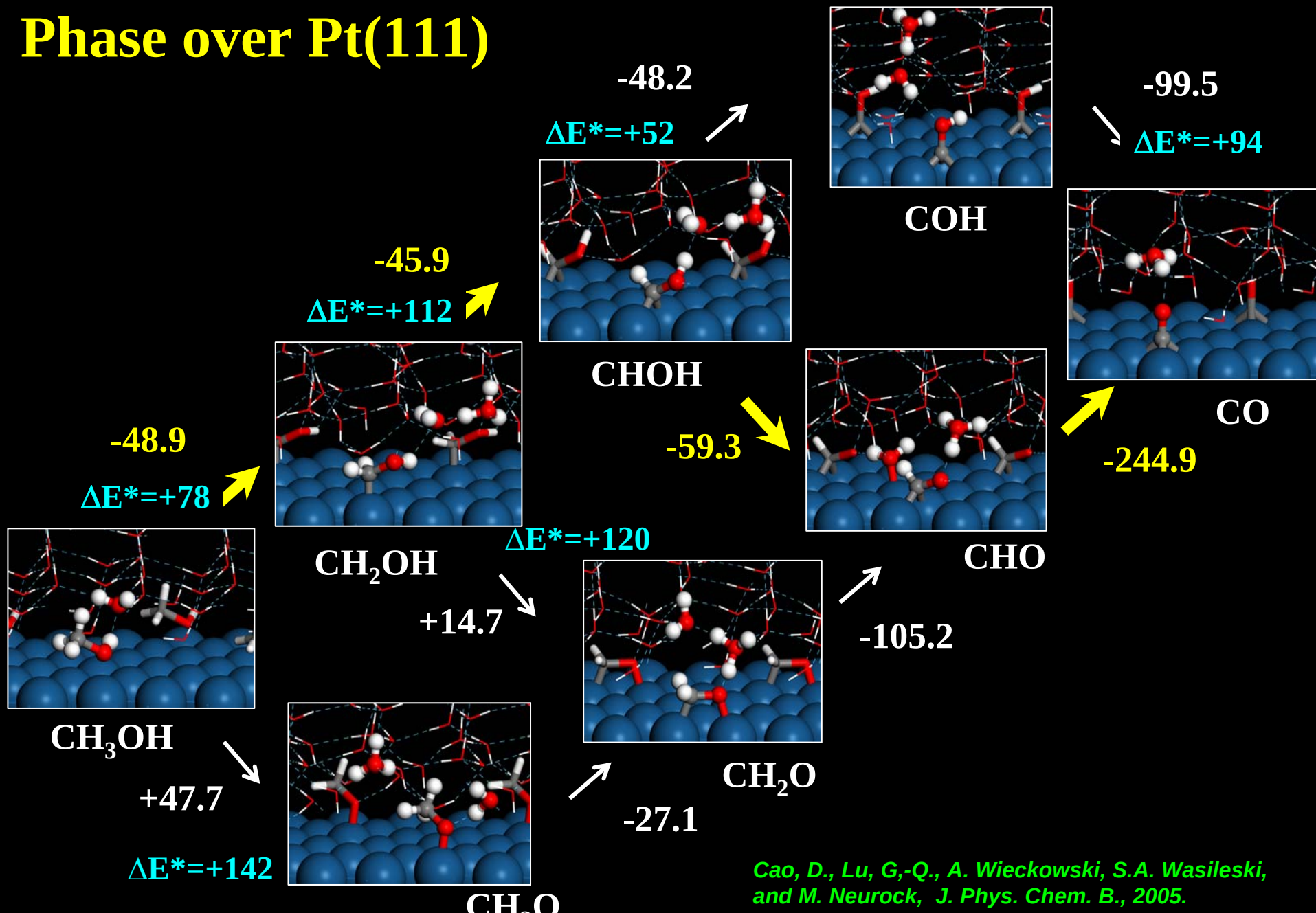

Cao, D., Lu, G,-Q., A. Wieckowski, S.A. Wasileski, and M. Neurock, J. Phys. Chem. B., 2005.

Methanol Dehydrogenation

Change in Potential

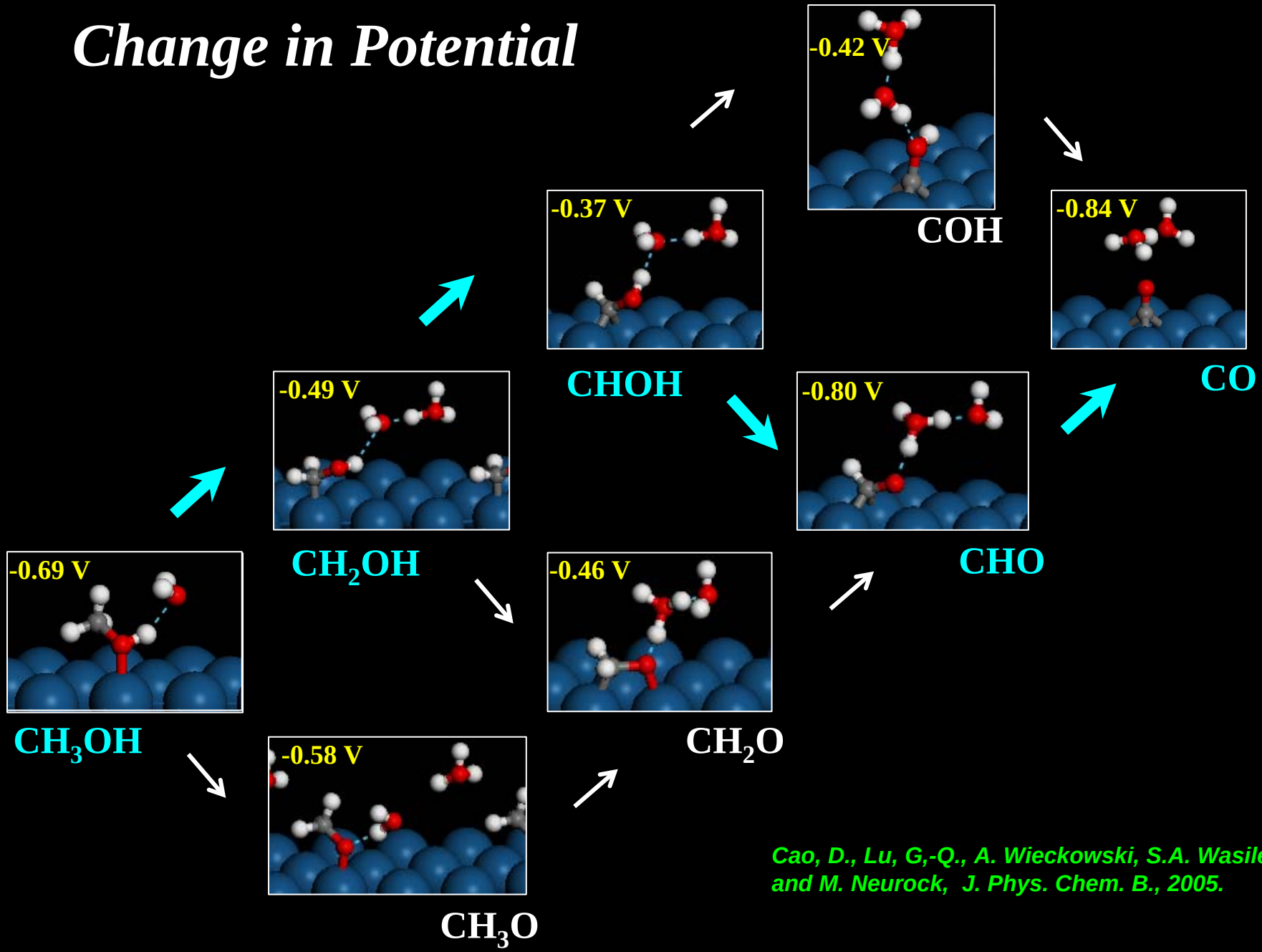

Cao, D., Lu, G,-Q., A. Wieckowski, S.A. Wasileski, and M. Neurock, J. Phys. Chem. B., 2005.

Ab Initio calculated potential dependent reaction energies for the activation of methanol to CH_2OH and CH_3O.

Energy vs. Potential

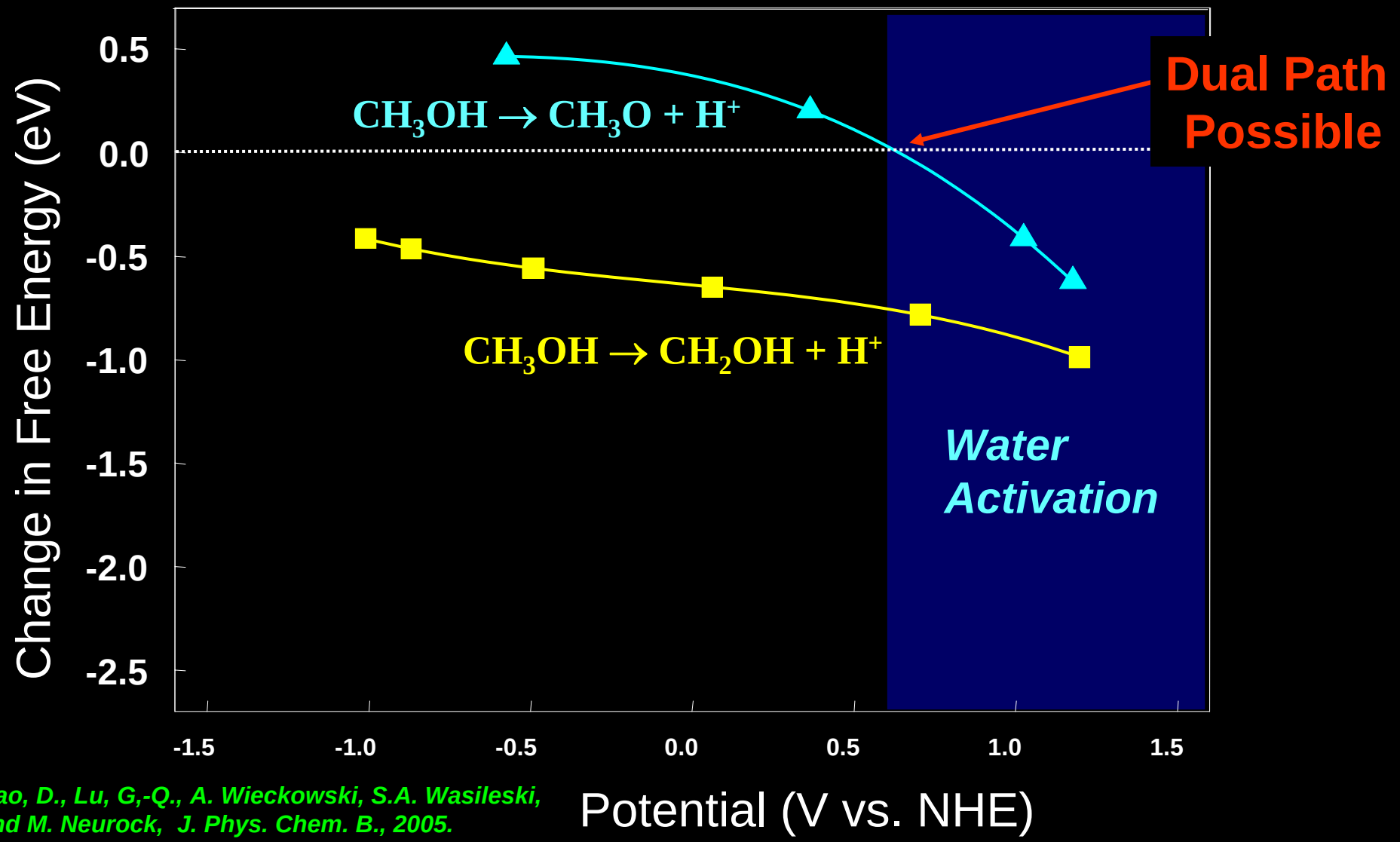

Cao, D., Lu, G,-Q., A. Wieckowski, S.A. Wasileski, and M. Neurock, J. Phys. Chem. B., 2005.

Subsequent CH_3O^* versus CH_2OH^* Activation

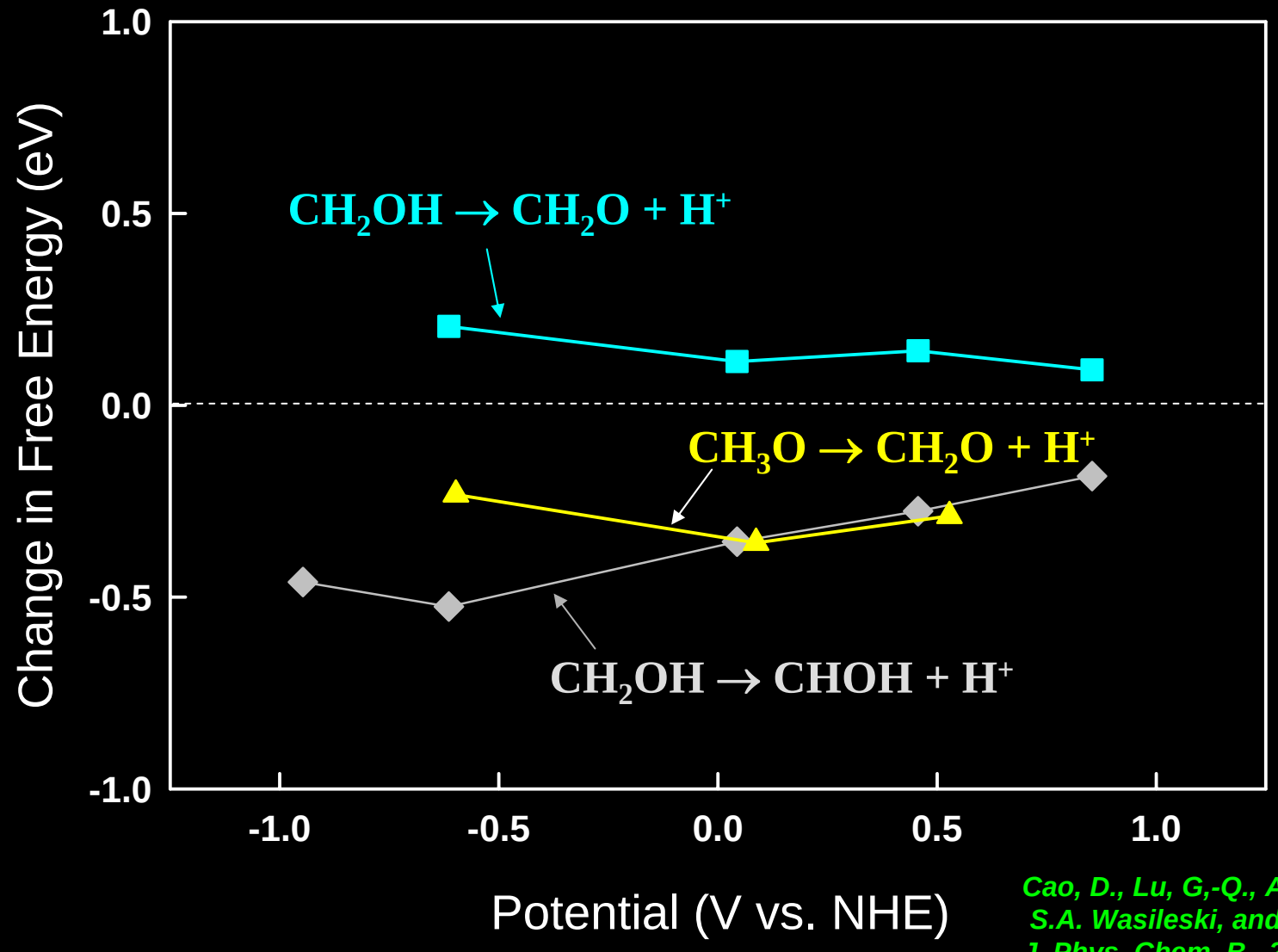

Cao, D., Lu, G,-Q., A. Wieckowski, S.A. Wasileski, and M. Neurock, J. Phys. Chem. B., 2005.

Electrocatalytic Methanol Dehydrogenation

Potential = +0.5 V vs. NHE

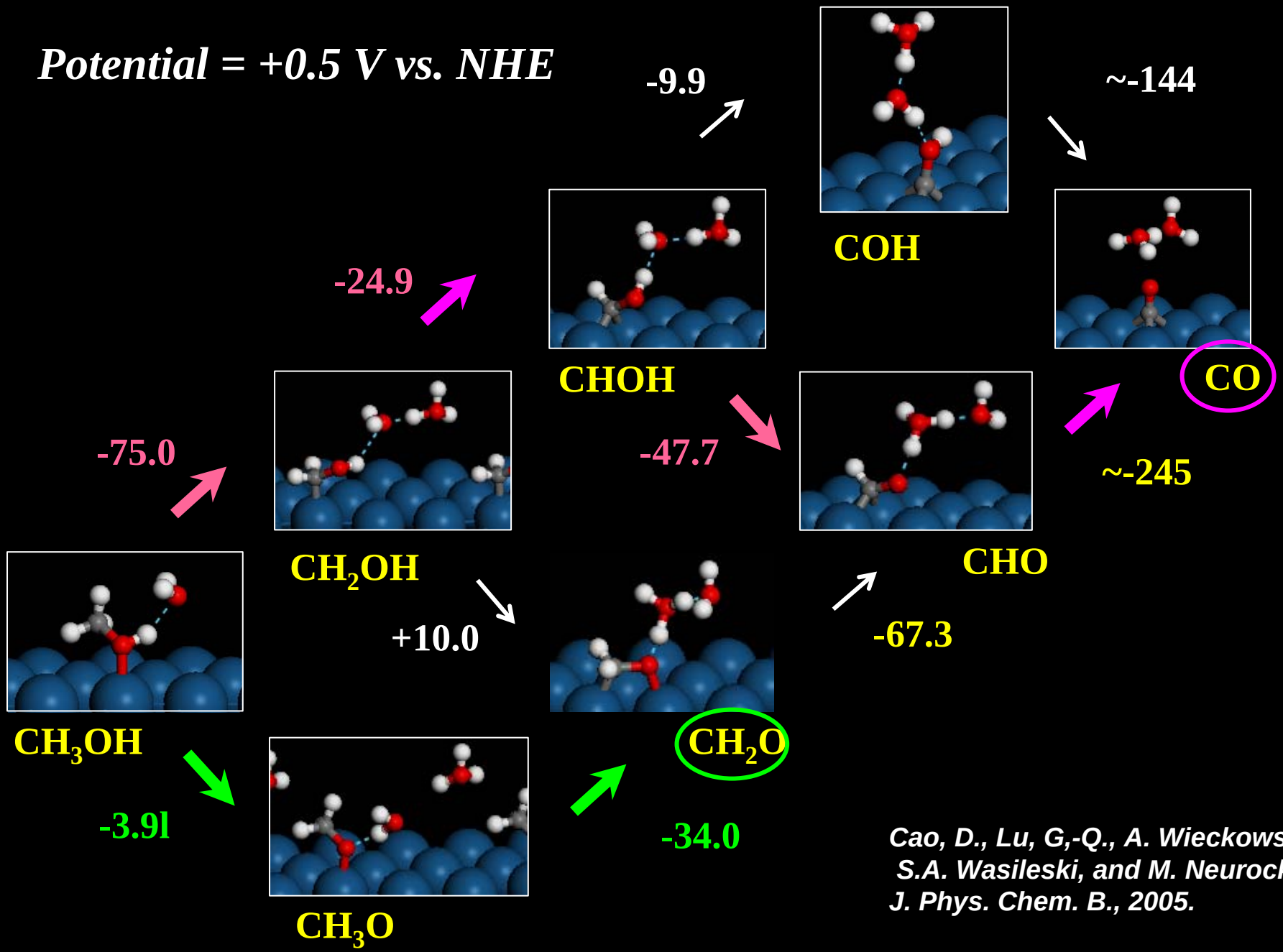

Cao, D., Lu, G,-Q., A. Wieckowski, S.A. Wasileski, and M. Neurock, J. Phys. Chem. B., 2005.

Periodic Trends for Methanol Activation

$$CH_3OH_{ad} \rightarrow CH_2OH_{ad} + H_{ad}$$

$$CH_3OH_{ad} \rightarrow CH_3O_{ad} + H_{ad}$$

	Co +0.41 -0.63	**Ni** +0.26 -0.45	**Cu** +0.55 -0.42
Ru -0.02 -0.40	**Rh** +0.03 +0.04	**Pd** -0.03 +0.38	**Ag** +0.80 +0.47
Os -0.10 -0.19	**Ir** -0.11 +0.22	**Pt** -0.27 +0.63	**Au** +0.48 +0.78

CH_xO Oxidation

Major Path is to form CO_2
Minor Path is to form Formic Acid or Formate

CO Oxidation

CO Oxidation over Pt(111)

Phase Diagram

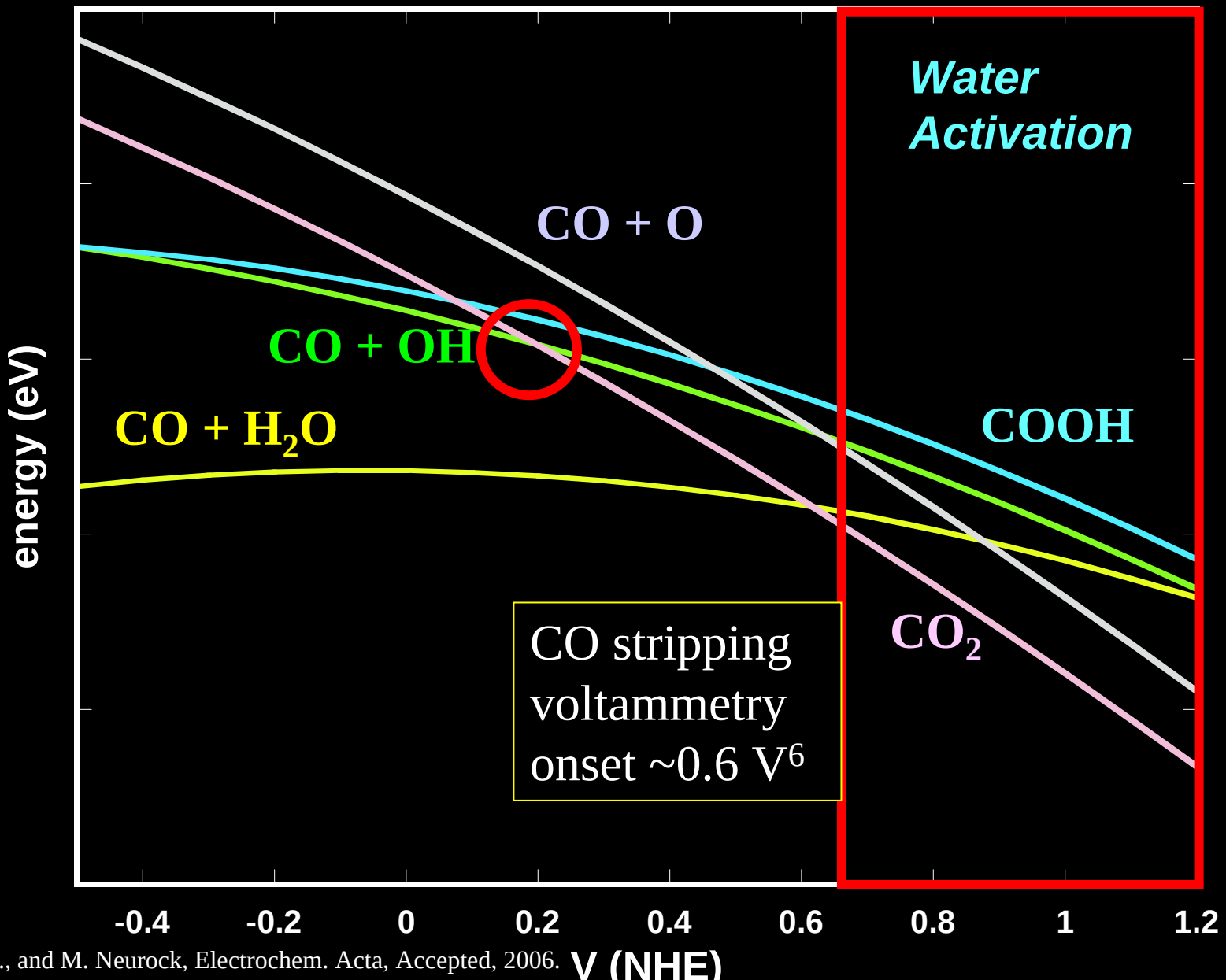

Janik, M.J., and M. Neurock, Electrochem. Acta, Accepted, 2006.

Simulated CO Stripping Voltammetry

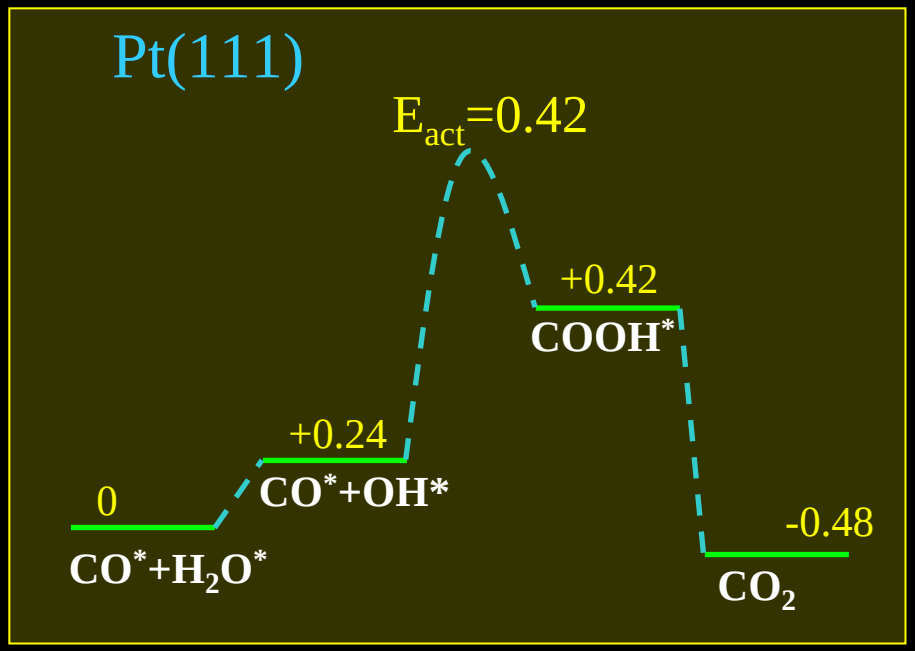

CO Stripping Peak Voltages (NHE)

mv/s	Expt.[8] polycrystalline	Expt.[8] Pt(111)	Sim.
5	0.68		0.734
20	0.73		0.779
50	0.78	~0.85	0.808

8 – Gasteiger et al. *J. Phys. Chem.* 98 (1994) 617.

Simulated CO Stripping Voltammetry

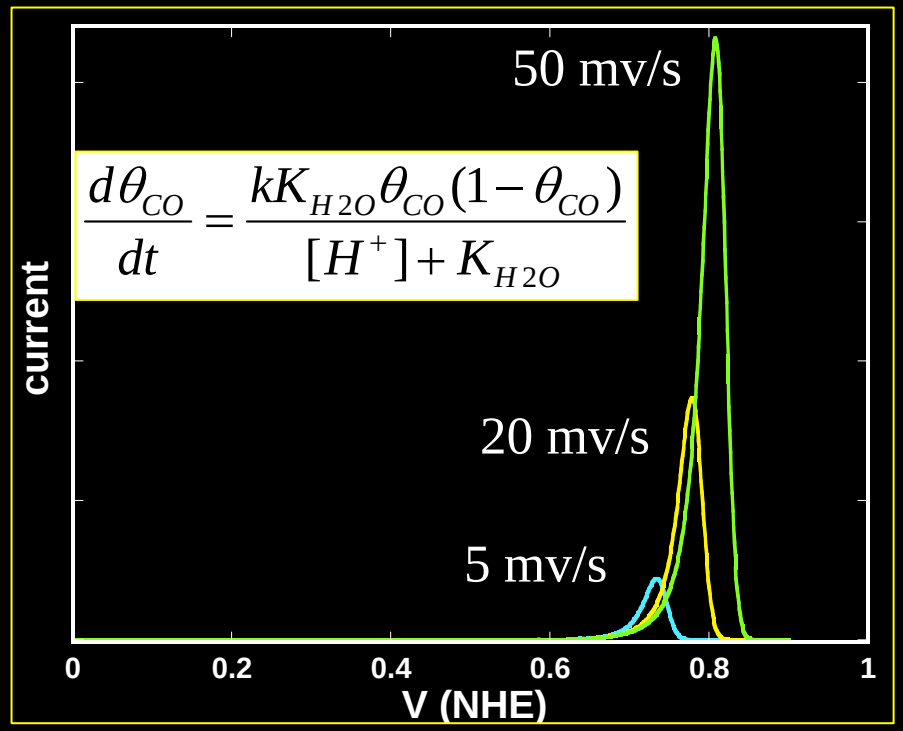

$$\frac{d\theta_{CO}}{dt} = \frac{kK_{H2O}\theta_{CO}(1-\theta_{CO})}{[H^+]+K_{H2O}}$$

CO Oxidation over Pt-Ru Alloys

Surface Models

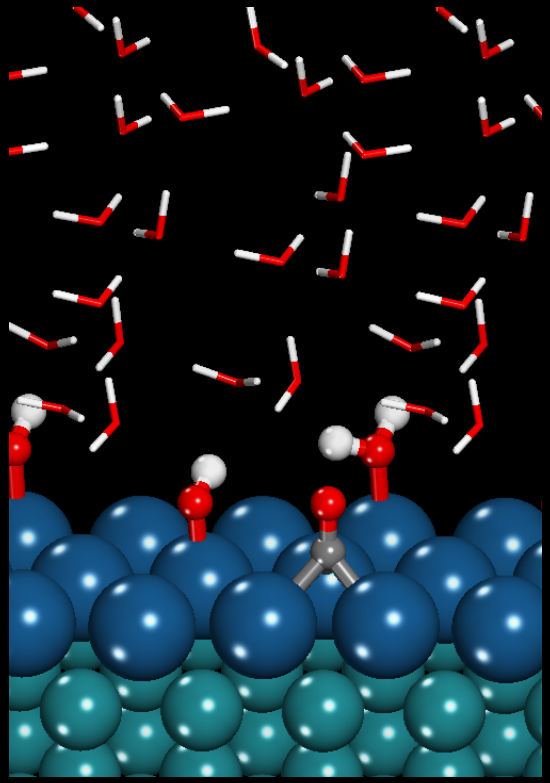

Overlayer
Pt surface over Ru

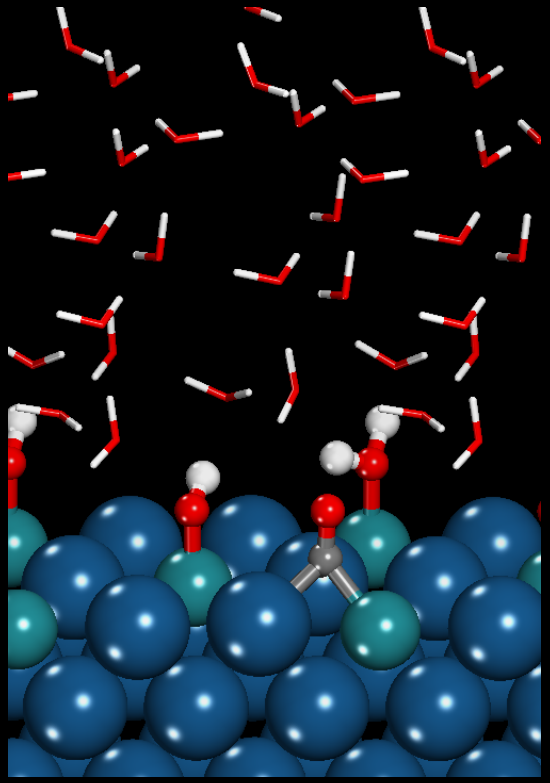

Surface Alloy
Ru well dispersed

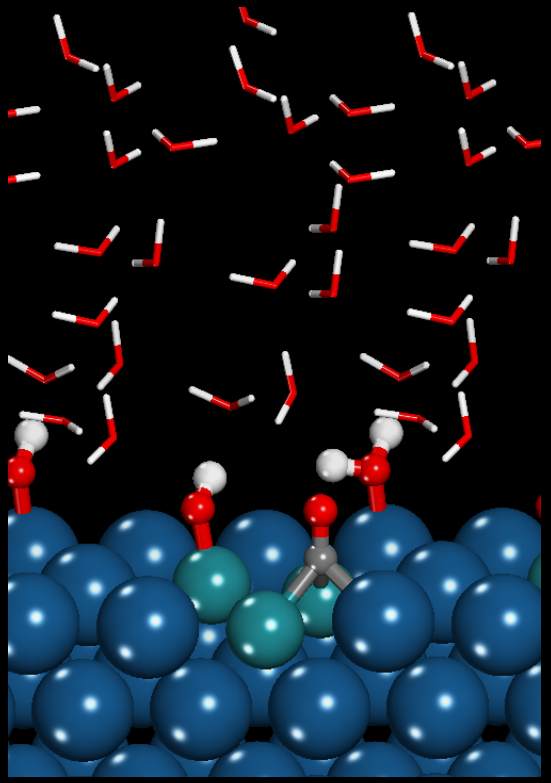

Surface Alloy
Ru islands

CO Oxidation over Pt-Ru Alloys

Equilibrium Potentials

	$H_2O \rightarrow OH$	$CO + H_2O \rightarrow CO_2$
Pt_{ML}/Ru(0001)	1.22 V	0.01 V
Pure Pt	1.29 V	0.55 V
Ru dispersed	0.74 V	0.66 V
Ru island	0.56 V	0.78 V

Ru dispersed in the surface greatly enhances water activation to OH.

Ru islands enhance water activation, but can form strongly bound O.

Pt/Ru overlayer weakens CO and H_2O binding to enhance CO oxidation.

CO Oxidation over Pt-Ru Alloys

Mixed Overlayer Model

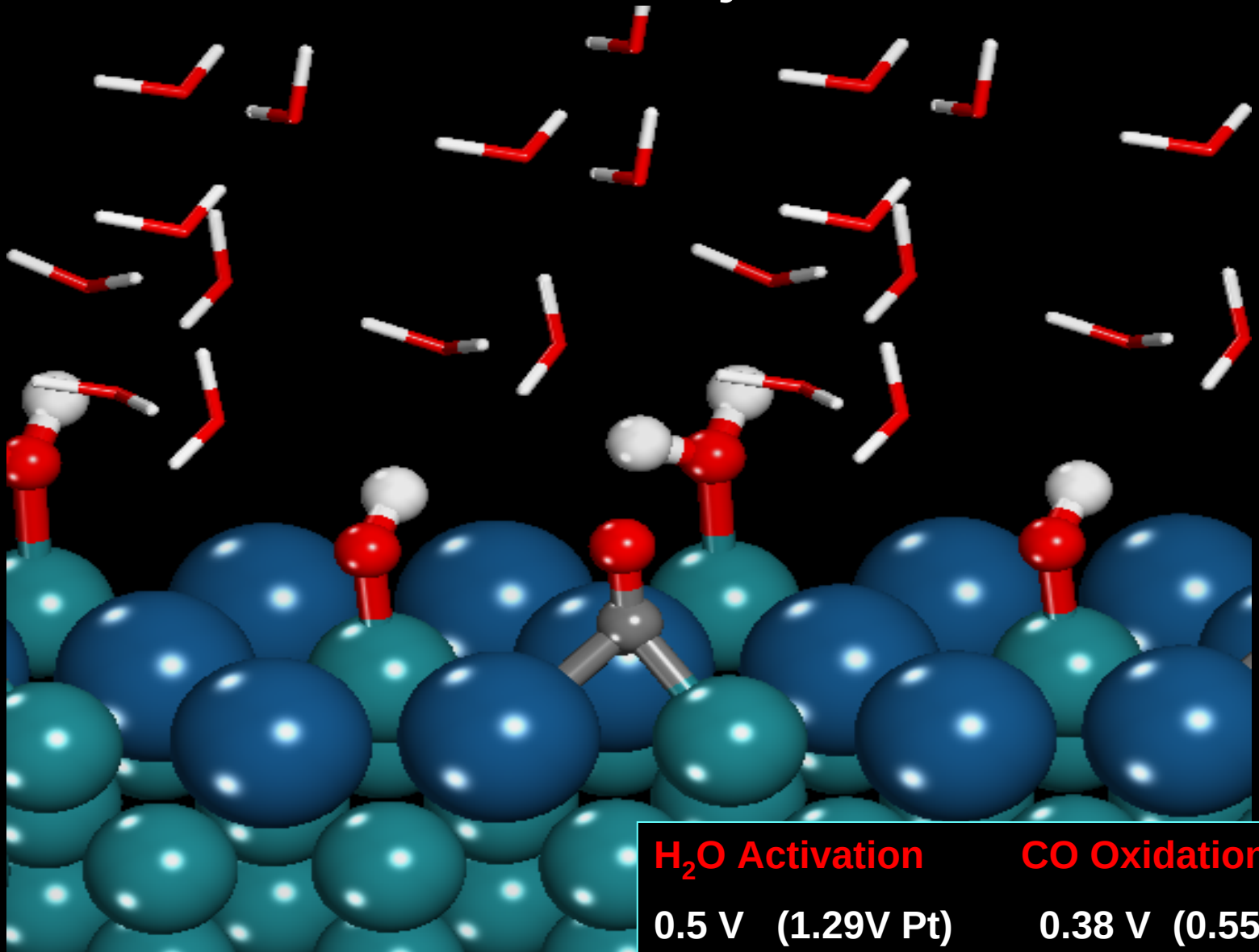

H_2O Activation	CO Oxidation
0.5 V (1.29V Pt)	0.38 V (0.55 V)

Pt-Ru Bimetallic Particle

40%Pt-60%Ru

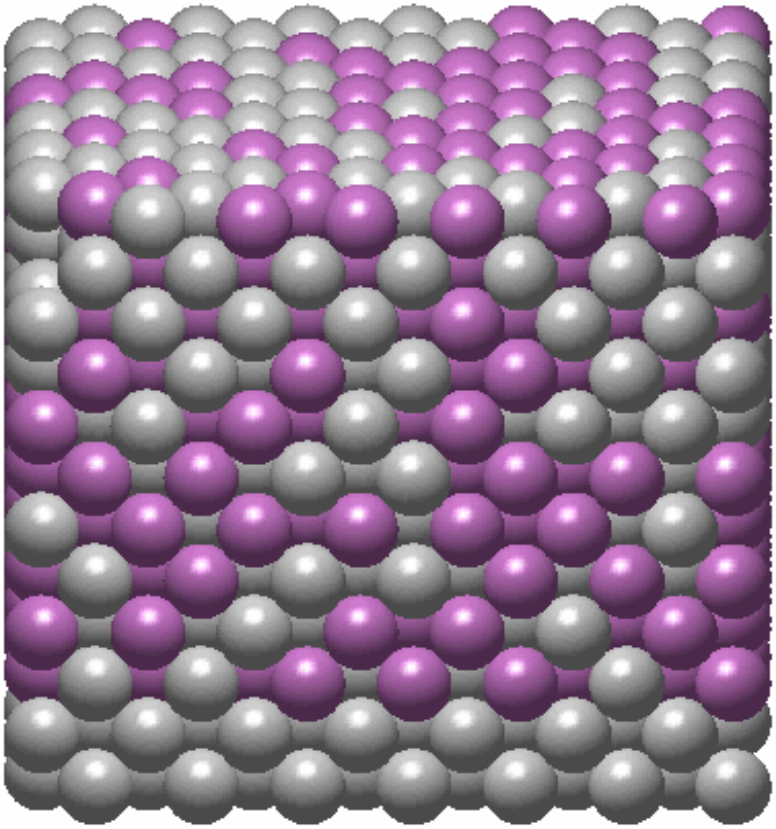

^{95}Pt-Pt/Ru Nanoparticles

Wieckowski, 2003

A Pt/Ru alloy surface shell!

(XRD)

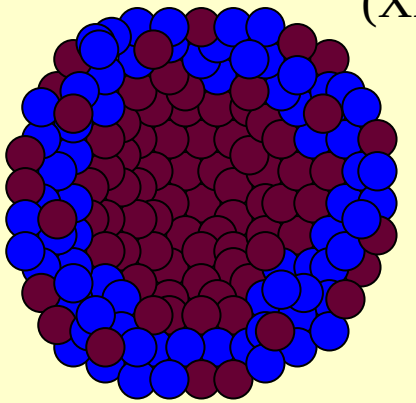

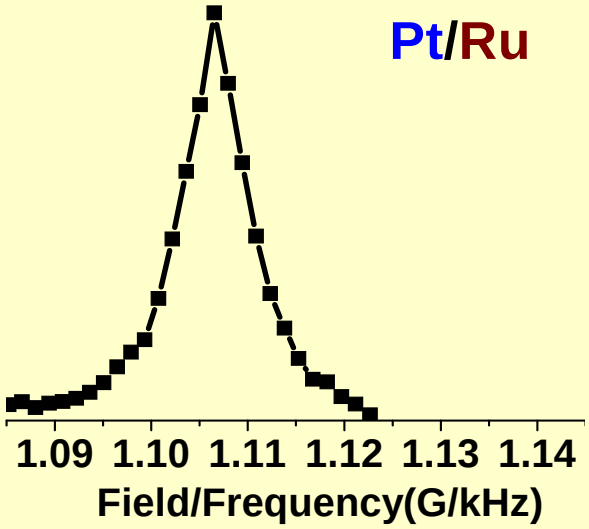

Theoretical Screening

Bimetallic Screening (Design)

Overlayer Systems

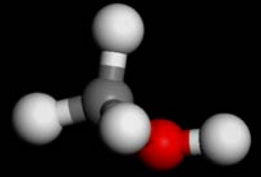

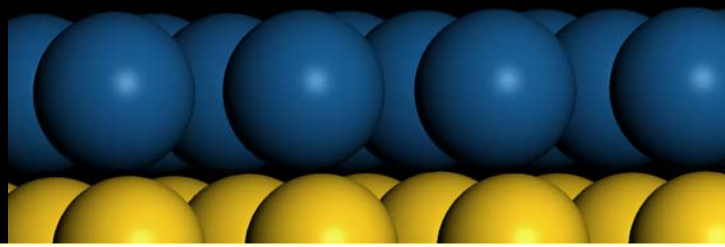

	$CH_3OH \rightarrow CH_2OH$	$CH_3OH \rightarrow CH_3O$	$H_2O \rightarrow OH$	$OH \rightarrow O$	$CO_{(gas)} \rightarrow CO_{ads}$	$CO+OH \rightarrow CO_{2(gas)}$
Pt(111)	-0.27	+0.63	+0.58	+0.04	-2.00	-0.07
Pt "skin" Ru(0001)	-0.07	+0.65	+0.73	+0.64	-1.27	-1.16
Pt "skin" Pd(111)	-0.34	+0.82	+0.67	+0.05	-2.01	-0.24
Pt "skin" Au(111)	-0.33	+0.40	+0.71	-0.35	-2.34	+0.14
Pt "skin" Al(111)	+0.45	+0.61				
Cu "skin" Zn(0001)	+0.62	-0.55	+0.84	+0.00	-0.85	-1.57
Au "skin" Cd(0001)	+0.45	+0.40	+0.35	+0.00	-0.36	-1.73
Ir(111)	-0.11	+0.22	+0.27	-0.12	-1.94	+0.23
Ir "skin" Cu(111)	-0.64	+0.68	-0.13	+0.23	-1.90	+0.29

Bimetallic Screening

Surface Alloy Systems

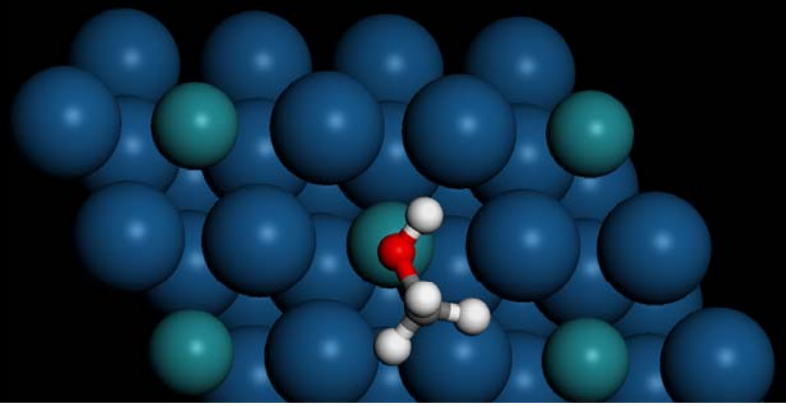

	$CH_3OH \rightarrow CH_2OH$	$CH_3OH \rightarrow CH_3O$	$H_2O \rightarrow OH$	$OH \rightarrow O$	$CO_{(gas)} \rightarrow CO_{ads}$	$CO+OH \rightarrow CO_{2(gas)}$
Pt(111)	-0.27	+0.63	+0.58	+0.04	-2.00	-0.07
Ru in Pt(111)	-0.20	+0.59	+0.42	-0.01	-2.20	+0.73
Pt in Ru(0001)	-0.01	+0.06	+0.25	-0.18	-1.77	+0.16
Sn in Pt(111)	+0.12	+0.94	+0.30	+0.70	-1.19	-0.62
Ni in Pt(111)	-0.26	+0.11	+0.64	-0.42	-1.99	+0.05
Ag in Pt(111)	-0.20	+0.52	+0.43	+0.36	-1.76	-0.29
Pt in Au(111)	+0.02	+1.00	+0.72	+0.95	-1.59	-0.67
Cu in Ir(111)	-0.29	+0.23	+0.13	+0.22	-2.21	+0.74
Ir in Cu(111)	-0.08	+0.48	+0.26	+0.27	-2.28	+0.50

Predicted Anode Ternary Alloys

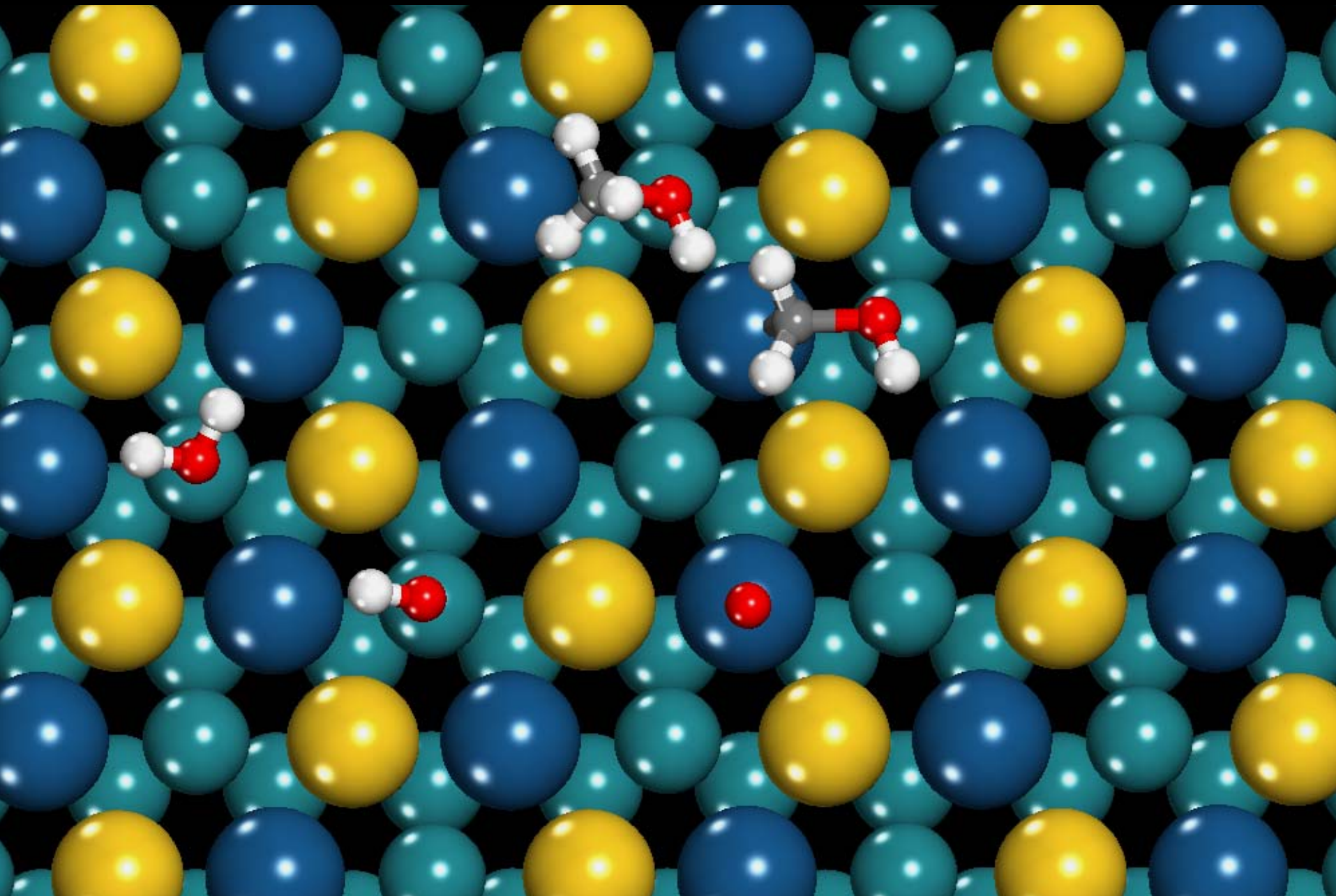

Predicted Anode Ternary Alloys

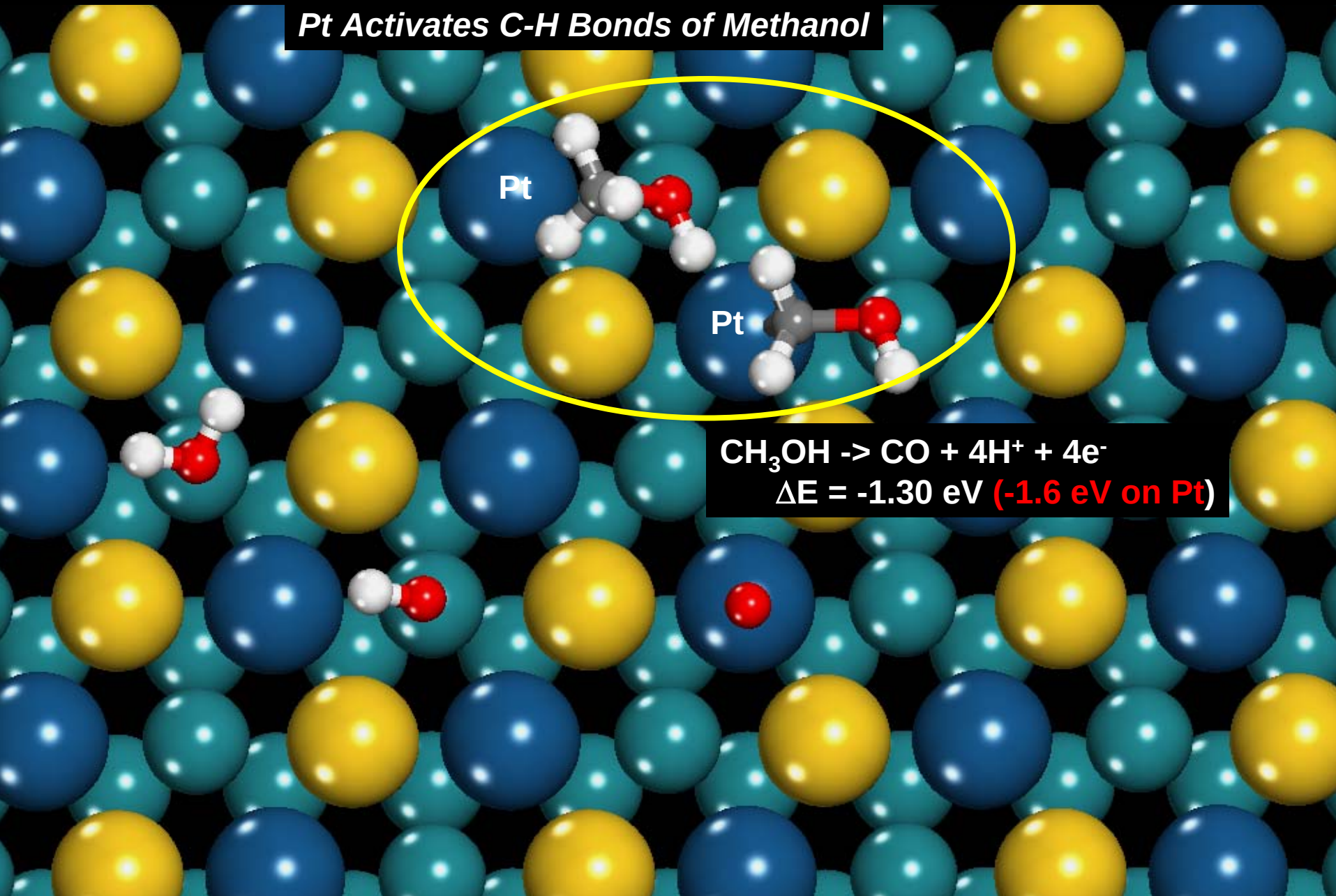

Surface Ru Activates Water

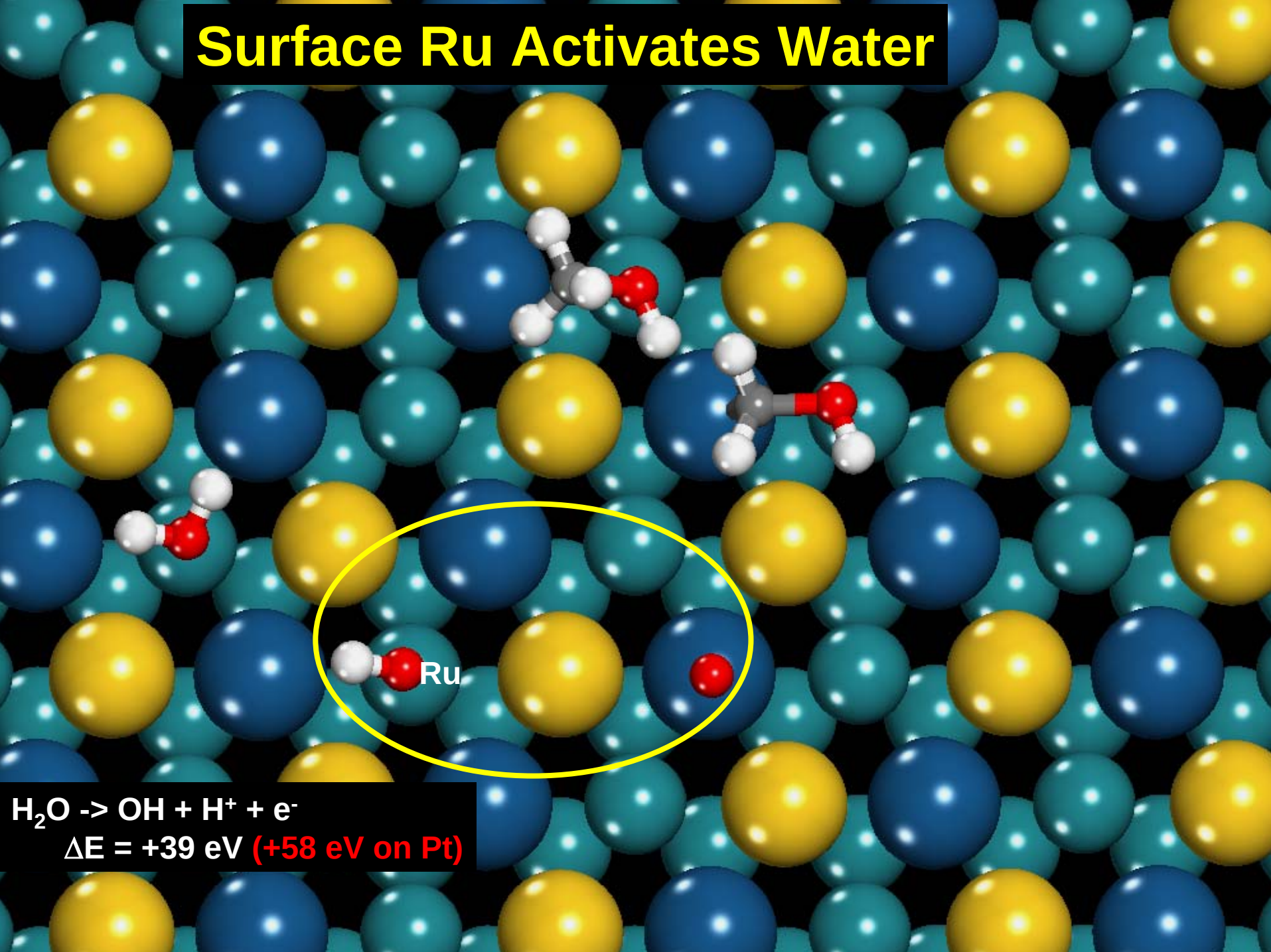

H_2O -> OH + H^+ + e^-

ΔE = +39 eV (+58 eV on Pt)

Subsurface Ru Weakens CO Adsorption

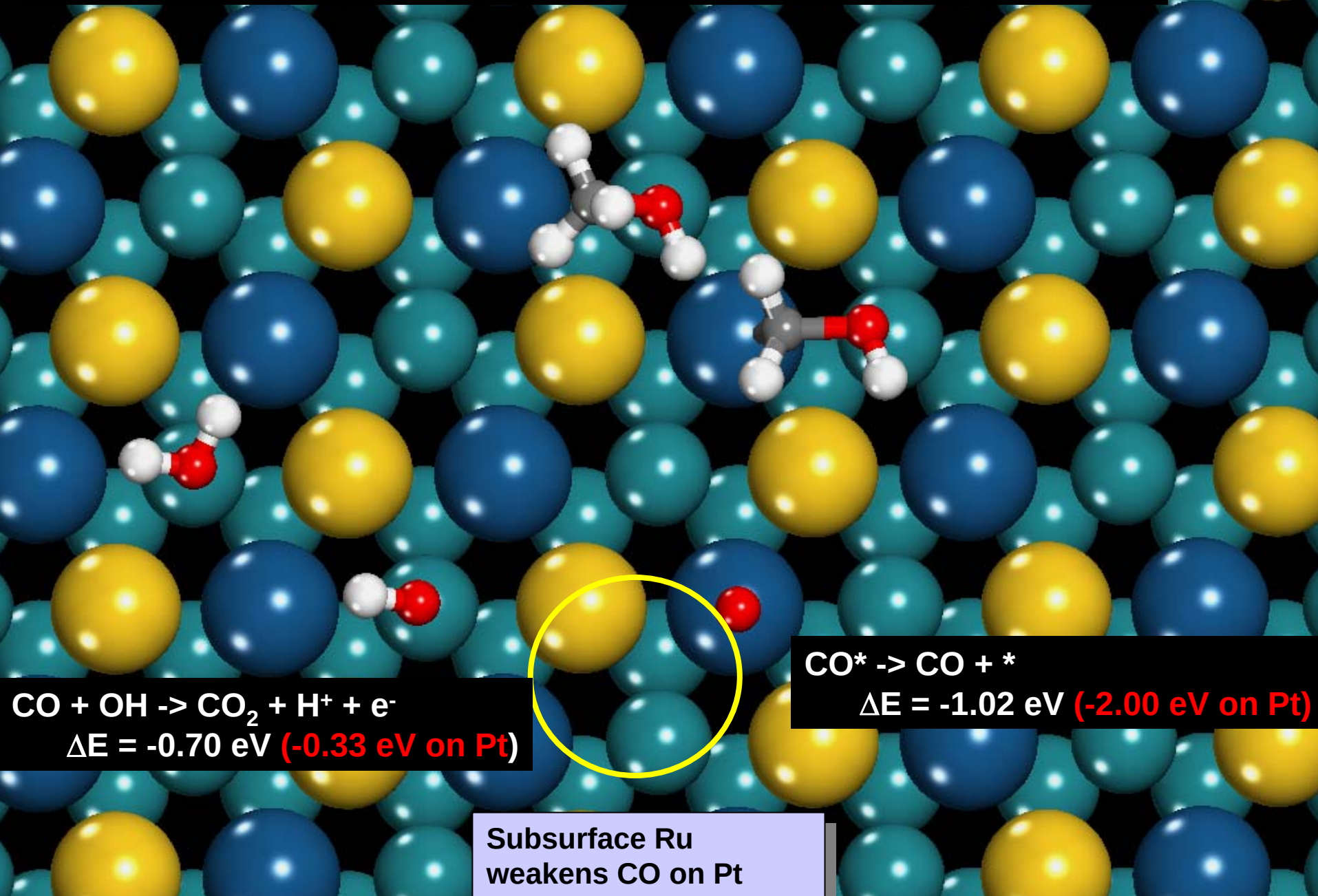

Au Weakens CO and Enhance CO Oxidation

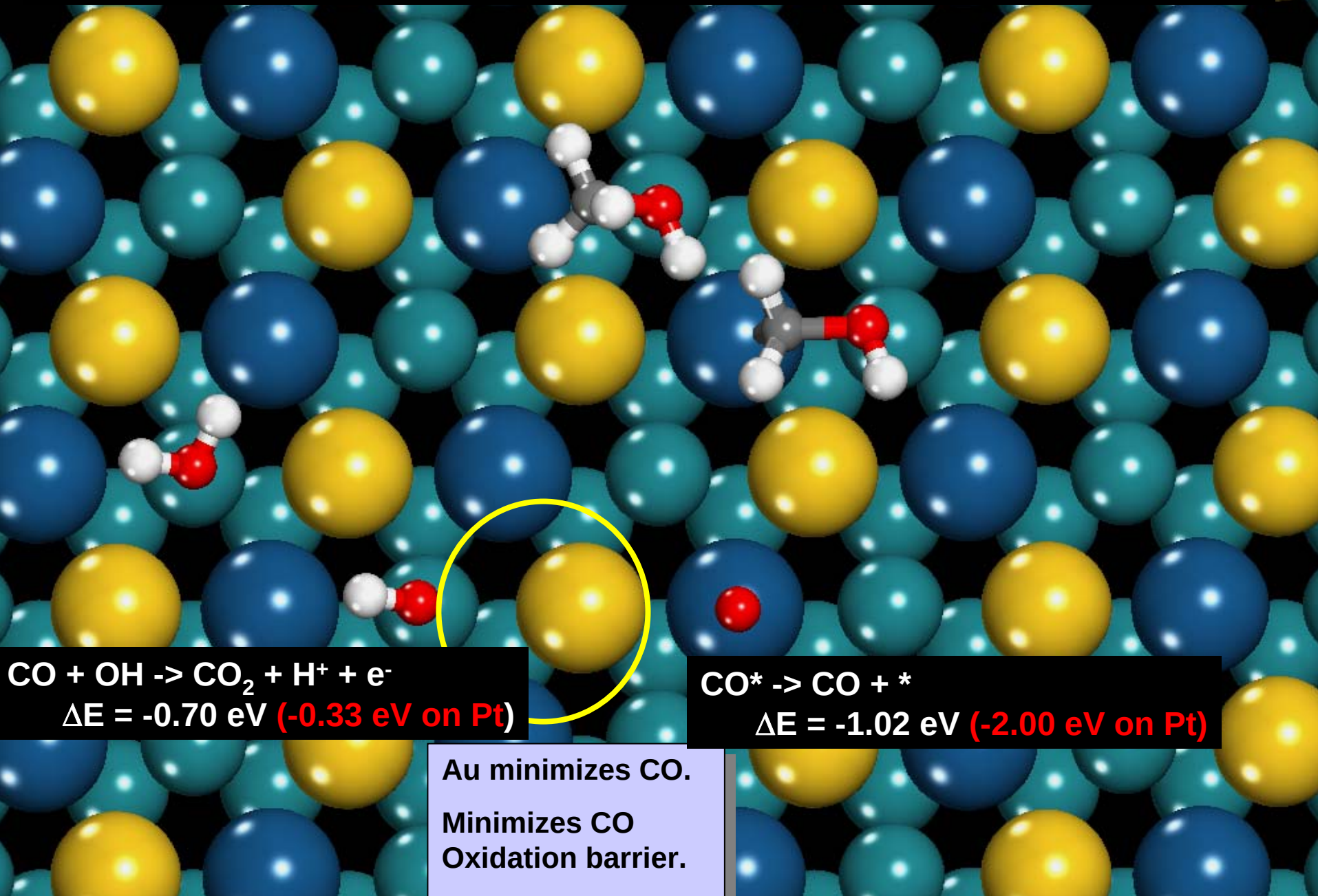

$CO + OH \rightarrow CO_2 + H^+ + e^-$

$\Delta E = -0.70$ eV (-0.33 eV on Pt)

$CO^* \rightarrow CO + *$

$\Delta E = -1.02$ eV (-2.00 eV on Pt)

Au minimizes CO.

Minimizes CO Oxidation barrier.

Synthesis?

Pt-skins well established.

Au segregation to the surface.

Pt-Au relatively immiscible.

Ru-Au miscible.

Currently being examined by JM and MURI Team (Wieckowski/Zawodzinski).

Janik, M.J., C.D. Taylor, and M. Neurock, Topics in Catal., Accepted, 2006.

Engineering the Reaction Environment

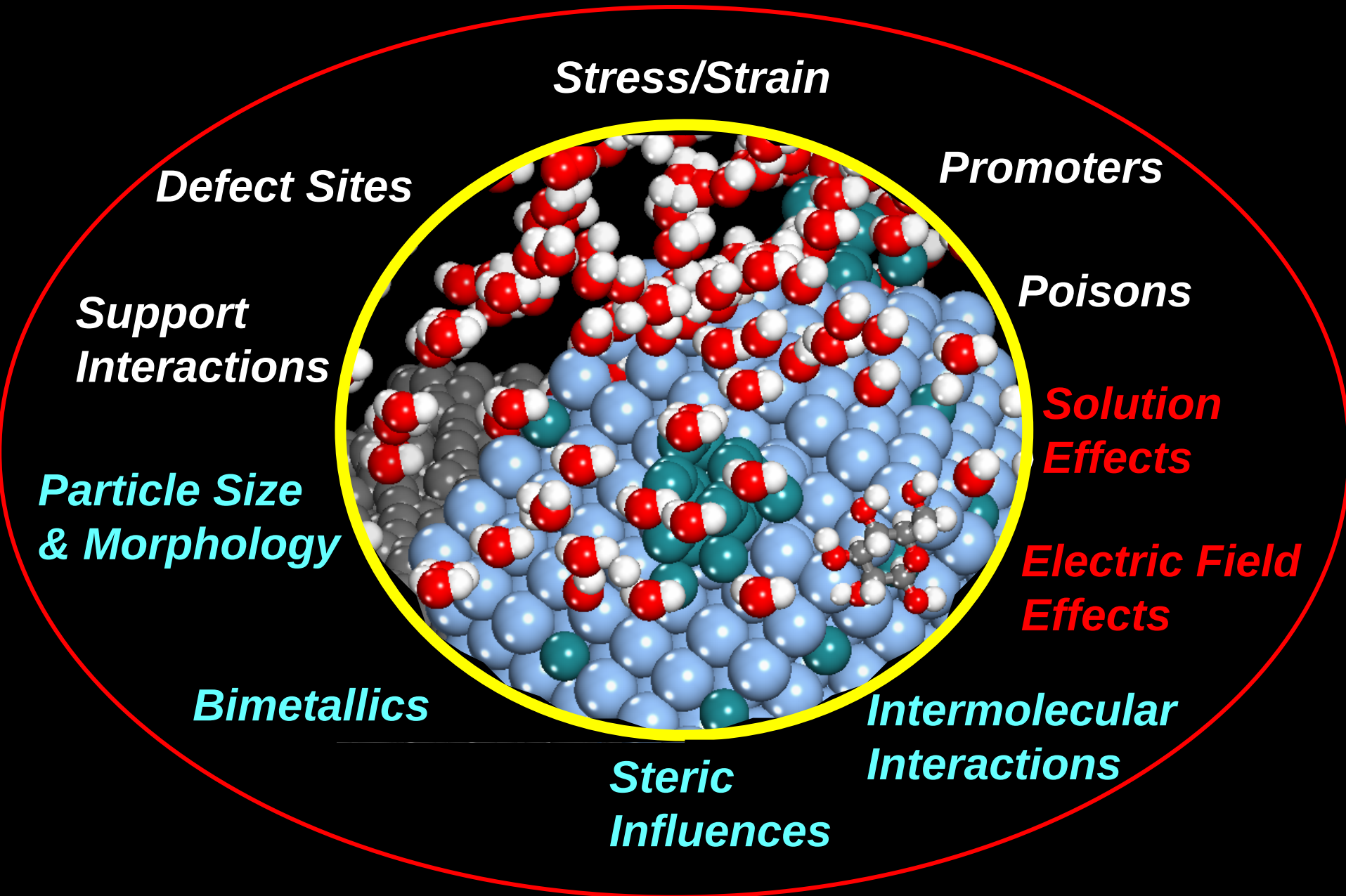

Future Challenges

Elucidating dynamic nature of the reaction environment.

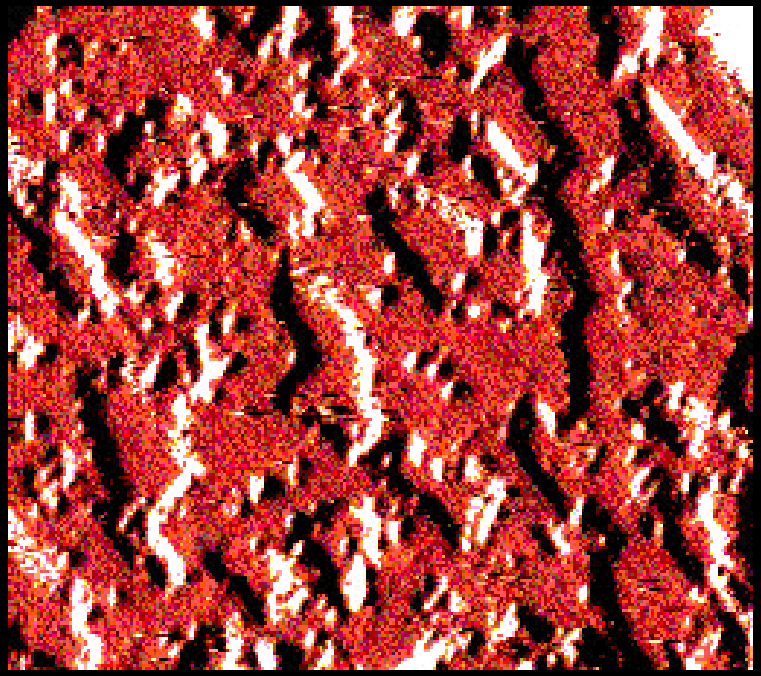

W. Roberts – Oxidation of Ammonia

Future Needs

Faster, cheaper, and more accurate methods.

Order N-Scaling, Improved Transition State Search Algorithms, Better DFT Functionals, Improved Property Prediction, Accurate Semiempirical Methods..

Ability to model more realistic reaction environments

Chirality, Defects, Promoters/Poisons, Solvents, Electric Fields Suports, Multimetallics, Multifunctional Materials.

Seamless integration between time and length scales.

Electronic, Molecular, Meso, Macro, and System Scales

Robust force fields for broad application of materials.

Reactive FF, Charge Transfer, Induced Polarization

Acknowledgments

Dr. Michael Janik
Dr. Chris Taylor
Dr. Sally Wasileski
Dr. Jean S. Filhol
Dr. Donghai Mei
Dr. Sanket Desai
Dr. Pallassana Venkataraman
Dr. Eric Hansen
Mr. Craig Plaisance

Army Research Office (MURI)
Department of Energy
National Science Foundation
Accelrys
DOE- NETL
Pacific Northwest Laboratory
Oak Ridge National Laboratory
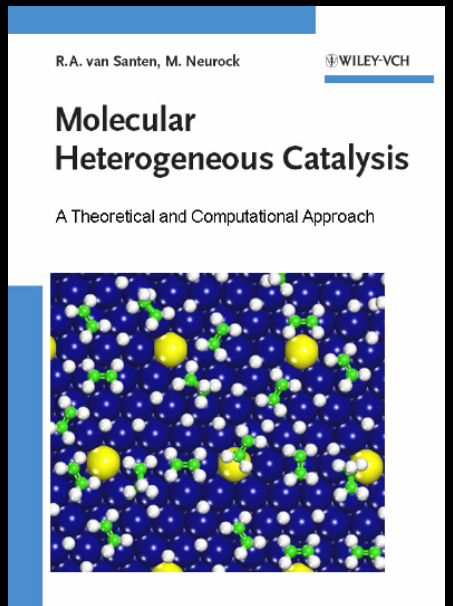
Professor Robert Davis (UVA)
Professor Rutger van Santen (TUE)
Professor Jens Nørskov (DTU)
Professor Andrzej Wieckowski (UIUC)
Professor Wilfred Tysoe (UWM)
Professor Enrique Iglesia (UC)
Professor Tom Zawodzinski (CWRU)